Innovative Infrastructure Solutions (2023) 8:268
https://doi.org/10.1007/s41062-023-01223-5

PRACTICE-ORIENTED PAPER

Fresh, mechanical and impact properties of self-compacting lightweight concrete containing waste PET fibers

Abdulkader Ismail Al-Hadithi[1] · Sara Ali Almawla[1] · Mahmoud Khashaa Mohammed[1]

Received: 9 June 2023 / Accepted: 18 August 2023 / Published online: 19 September 2023

Abstract

The aim of this study is to evaluate fresh, mechanical, and impact resistance of structural lightweight self-compacting concrete with good thermal insulation and incorporating waste PET fibers with different volume fractions and aspect ratios. Integration of the characteristics of self-compacting concrete, which are followability, good strength and sustainability with the characteristics of lightweight concrete, represented in reducing the loads of the structure and thermal insulation, in addition and with reducing the environmental damage represented by plastic by utilizing a fiber is the goal of this research. As a first stage of this study, lightweight Ponza aggregate was used as a coarse aggregate, as four reference mixtures were produced with volume replacement ratios of coarse aggregate volume ranging from 20 to 100%, and a reference mixture was produced for the purpose of comparison. In the second stage of this study, the performance of self-compacting lightweight concrete SCLC reinforced with waste PET fibers were analyzed in terms of fresh, physical, mechanical, and thermal properties as well as its flexural toughness and impact behavior. Nine different fiber reinforced self-compacting lightweight concrete were designed using waste plastic fibers WPF at three different volume fraction (0.5%, 0.75%, and 1%) and three different aspect ratio (15, 30, and 45). After design process, similar properties in the first stage in addition to toughness and impact test were performed. The results of second stage verified that the adding WPF to SCLC leads to reduction in dry density, ultrasonic pulse velocity, and thermal conductivity around 9%, 14%, 19%, respectively, with increase in PET fibers ratio from 0 to 1% at aspect ratio of 45. Further, the result of flexural toughness test showed that the use of WPF in SCLC leads to an interesting improvement in the post-cracking performance and enhanced ductility of concrete. Furthermore, there is substantial improvement in impact resistance of all WPF-reinforced SCLC mixes over control mix. Results clarified that WPF concrete mix of volume fraction 1% and aspect ratio 45 gave the best impact resistance, the improvement of its impact resistance at ultimate failure over control mix was 373.3%.

Keywords Self-compacting lightweight concrete · Impact · Waste PET fibers · Mechanical properties

Introduction

Concrete is considered as one of the most used construction materials worldwide. This is due to the availability of its basic compounds in nature, its cheap price, its durability and its easiness of pouring and molding. Conventional concrete normally needs vibration process through the production stage and this can be considered as one of the limitations to be used for concrete members with heavy reinforcement. Another limit is the self-weight of concrete. The use of self-compacting lightweight concrete SCLC has many benefits in terms of: (i) reducing the loads on the structures, which leads to reducing the section dimensions of the structural concrete members (ii) eliminating the required vibration. Based on the foregoing, a new approach in concrete and construction technology has been adopted to produce lightweight (LW) and self-compacting (SCC) concrete at the same time [1, 2].

Okamora created SCC in Japan in 1988 to solve the issue of concrete durability, which arises from insufficient compaction in the absence of experienced laborers [3]. In addition to being self-compacting, which lessens vibrator

✉ Abdulkader Ismail Al-Hadithi
abdulkader.alhadithi@uoanbar.edu.iq

Sara Ali Almawla
sar17e111@uoanbar.edu.iq

Mahmoud Khashaa Mohammed
mahmoud.mohammed@uoanbar.edu.iq

1 Civil Engineering Department, College of Engineering, University of Anbar, Ramadi, Iraq

noise pollution and lowers placing costs, it also has excellent deformability, which makes it easier for concrete to flow through constrained spaces and encapsulate reinforcement without bleeding or cement paste and aggregate separation. The SCC's low yield value for high deformability and moderate viscosity for resistance to segregation and bleeding are the causes of these advantages [4, 5]. Moreover, there was an improvement in the durability of the SCC in terms of sulfate attack, fire resistance, chloride penetration and carbonation) as indicated by De Schutter et al. [6].

There is another versatile type of concrete called lightweight concrete. It has created unlimited interest and great industrial demand in construction projects for the unique benefits achieved by reducing the weight of the concrete. In addition to the decreased inertial seismic forces as a result of reduced dead loads, which makes buildings with LWC more preventive protections against the earthquakes.

Because of the LWC's strong thermal insulation and low thermal conductivity, its fire resistance is more comparable to that of regular concrete [7, 8]. Under EN 206-1 [9], concrete and aggregates shall be lightweight when the oven-dry density is more than 800 kg/m^3 and not exceed 2000 kg/m^3 and either oven-dry particle density is less than 2000 kg/m^3 or loose oven-dry bulk density is less than 1200 kg/m^3, respectively [9].

The most popular type of LWC is lightweight aggregates concrete (LWAC), which can be produced using either lightweight coarse aggregates or lightweight coarse aggregates combined with natural fine particles [10, 11].

Self-compacting lightweight concrete (SCLC).

SCLC is relatively a new generation and breakthrough in the field of high-quality concrete. The precise design and proper production methods of the SCLC are still difficult challenges of high-quality requirements, comprising a revolution in the technology of concrete science. SCLC does not only combine the favorable properties of both the SCC and LWAC, but also limits the negative properties of them [12].

Due to the lightweight aggregate's tendency to float on the top and form a weak layer, especially in combinations with high consistency, LWAC exhibits observable issues in its freshly formed stage, necessitating specific attention in accordance with workability considerations. This issue gets worse when LWAC is vibrated improperly. Therefore, where there is no requirement for external vibration, it is advised to incorporate lightweight aggregate into SCC [13, 14].

The simplest strategy to lower the self-weight of the concrete and to receive all the benefits of LWC in addition to those from SCC is to substitute lightweight aggregate for regular aggregate in the mix design of SCC. The new product (SCLC) could have good quality and excellent segregation resistance. Since lightweight aggregates were all produced from natural stones in the past, techniques for the manufacturing of artificial lightweight aggregate have been developed as a result of its scarcity in various locations. Artificial lightweight aggregate is made from industrial waste products like blast furnace slag and fly ash [15]. Some researchers used natural lightweight aggregates [1, 5, 15] to produce SCLC while the majority resorted to the use of artificial lightweight aggregates.

Thermal properties of self- compacting lightweight concrete

Due to rising energy prices and the scarcity of natural resources, the global energy crisis has emerged as one of the main issues. As a result, it has become crucial to include energy saving measures in the building code. A thorough understanding of the thermal characteristics of the building materials is necessary for the construction of energy-efficient buildings. In all climatic zones of the world, concrete is the material most frequently used for building structure. The thermal properties of concrete are crucial for determining how well concrete will operate over time, so they should be taken into account [16].

Fibers in self-compacting lightweight concrete

Many of concrete buildings may be cracked due to weakness of the concrete to resist tensile forces. Fibers can be used to mitigate this weakness problem and to enhance certain properties of concrete by absorbing energy up to fracture [17].

The disadvantages of lightweight aggregates include low strength and high absorption capacity. Additionally, for the same compressive strength, lightweight aggregate concrete is more brittle than conventional weight concrete. Therefore, it is crucial to incorporate fibers into the SCLC mix design [18]. Numerous studies have proposed the use of fibers in LWAC and SCC [19, 20]. However, there have only been a few studies done on the use of waste Polyethylene Terephthalate (PET) fibers in SCLC.

Use of polyethylene terephthalate (PET) as fibers in concrete

PET is a semi-crystalline (white and opaque) thermoplastic polymer made when terephthalic acid and ethylene glycol undergo an esterification or transesterification reaction, with water or methanol as a byproduct [21]. The consumption of PET has been growing quickly worldwide, which has increased PET trash. Creative ways to reuse used PET bottles are being looked for where they might be used in large quantities in order to reduce the pollution threat caused by the presence of a large volume of PET garbage in landfills. One such method of reuse has been in concrete mix designs, where it can be utilized as fiber or aggregate [22]. Many researchers studied the effect of adding PET wastes on the shear strength of reinforced concrete [23] and flexural strength [24]. Some researchers also studied the effect of temperatures on the behavior of concrete containing plastic waste when exposed to high temperatures [25].

Al-Hadithi et al. [26] published a study on the impact behavior of slab concrete reinforced with PET fibers in 2018. Typical concrete slabs with different PET fiber volume fractions (0%, 0.5%, 1%, and 1.5%) were tested using the low velocity impact test. According to the study's findings, adding PET fibers greatly increased impact resistance in particular, 1.5% addition. Al-Hadithi et al. [27] in another study assessed the impact resistance of SCC slabs reinforced with PET fibers in 2019. Several volumetric ratios from 0.25 to 2% were employed to examine slab behavior. Experiments show that the compressive and flexural strengths of SCC mixes are improved by the addition of PET fibers. De Silva and Prasanthan's experimental work in 2019 [28] stated that the inclusion of PET fiber within the concrete mixture increased energy absorption capacity, which means better impact resistance and improved flexural capacity until first crack. Recent development in using waste materials such as waste glass in ultra-high-performance concrete has been studied extensively by Tahwia and et al. [29, 30].

The literatures about SCLC reinforced with fiber still have a lack of knowledge to be fulfilled, this current study aims to contribute in accomplishing this gap regarding the properties of SCLC reinforced with waste plastic fibers WPF such as fresh, thermal, and hardened properties focusing on post-cracking performance under bending load and impact behavior. Also, the use of different volumetric WPF ratios in Ponza lightweight self-compacting concrete with different aspect ratio can be considered a recent research field that has not been previously explored.

Experimental program

Materials

The materials used to produce concrete mixes in this study are: Ordinary Portland cement (OPC) type I was used for preparing all concrete mixes in this study. Cement properties is complying with the requirement of Iraqi standard specification (I.Q.S) No.5/1984 [31]. The physical and chemical specifications of cement are listed in Table 1. Fly ash is a byproduct fine powder left from burning pulverized coal in plants of electric power [32]. It was incorporated in the SCC to supplement the cementing features and to enhance the overall performance of mixes like workability, strength, and microstructure [33]. In the current study, fly ash with a Blaine fineness of 380 m^2/kg was used as a secondary binder to reduce consumption of cement as well as emission of CO_2. Based on chemical composition provided by the supplier, see Table 1, the powder consists of approximately 40% Silicon dioxide, 15% Aluminum oxide, and 20% Iron oxide. Therefore, fly ash could be classified as Class F according to ASTM C618-12a [32]. Locally available natural sand with particle size in the range of (0–4.75) mm constituted the fine aggregates for all mixes. The physical properties of fine aggregate and sieve analysis are given in Table 2 and Fig. 1, respectively. The grading of this aggregate confirms the limitation of ASTM C33-13 [34].

Coarse aggregate: Normal weight aggregate with 12.5 mm maximum size crushed gravel was employed as normal weight coarse aggregate in this study. Tables 3 and Fig. 2 list its physical properties and grading curve for coarse aggregate, which confirms the specifications of ASTM C33-13 [34], respectively. All tests were conducted in the engineering materials laboratory /University of Anbar.

Table 1 chemical and physical properties of Portland cement and fly ash

Component (% content)	Cement	Fly ash
CaO	61.95	18.1
SiO_2	20.91	38.8
Al_2O_3	5.31	14.7
Fe_2O_3	3.33	19.48
SO_3	2.5	1.5
MgO	2.35	3.3
K_2O	0.92	1.79
Na_2O	0.17	0.38
Specific gravity	3.15	2.1
loss on ignition	2.08	1.38
Insoluble residue	0.96	–
Lime saturation factor	0.91	–
Setting time (Vicat method),(hour: minutes)		
Initial setting	2:20	–
Final setting	4:14	–
Compressive strength, MPa		
3th day	16	–
7th day	28	–

Table 2 Physical, chemical properties of fine aggregate

Property	Results
Specific gravity (SSD)	2.64
Water absorption%	0.81
Dry loose unit weigh(kg/m^3)	1796
Sulfate content SO_3	0.19
Fineness Modulus	3.3

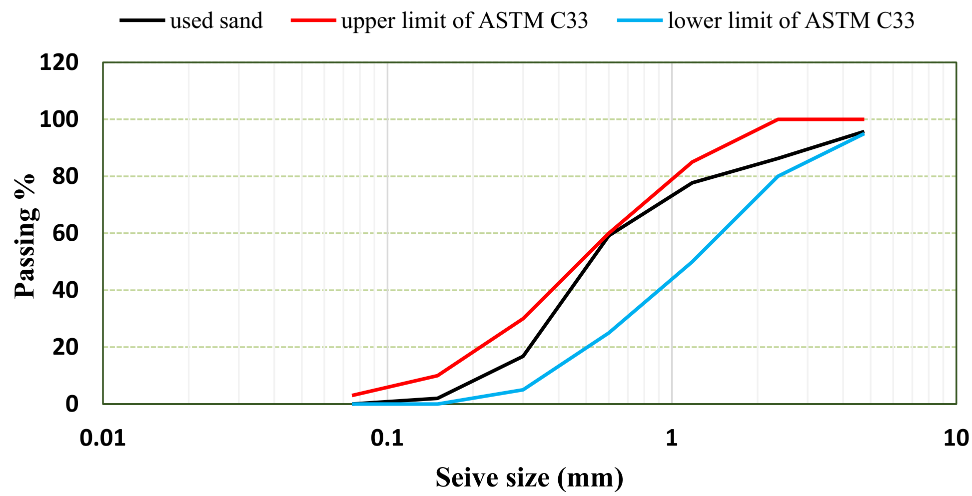

Fig. 1 Grading curve of fine aggregate

Table 3 Physical, chemical properties of normal weight coarse aggregate

Property	Results
Specific gravity (SSD)	2.67
Water absorption%	0.53
Dry loose unit weigh (kg/m^3)	1553
Dry rodded unit weight (kg/m^3)	1581
Sulfate content SO_3	0.05
Fineness Modulus	5.9

Lightweight coarse aggregate: Aggregates of clayey stone called Ponza used as lightweight aggregate to decrease self-weight of concrete mixtures. The aggregates were crushed and sieved to the desired gradient complying with the requirement of ASTM C330-17 [35] as shown in Fig. 3. Laboratory tests conducted to find the physical properties of the aggregates like specific gravity and absorption, which are listed in Table 4. In order to eliminate the slump loss due to high capacity of water absorption induced from cellular structure of the lightweight Ponza aggregate the following procedure was implemented. Lightweight Ponza aggregate was first immersed in water for 24 h. Afterward, the excess water was dripped off and the aggregate spread out by hand in laboratory for having a saturated surface dry condition (SSD). Figure 4 shows photographic views of the Ponza aggregate spread out inside laboratory.

Superplasticizer: Paste of SCC requires high deformability to prevent increases in the internal stress induced from contact between coarse aggregate particles. High deformability of SCC can be attained only by the employment of a Superplasticizer (SP), that decreases the water-powder ratio to a very low value [3]. In this investigation aqueous solution of modified Polycarboxylic based on high range-water reducing agent (HRWRA) was employed as superplasticizer

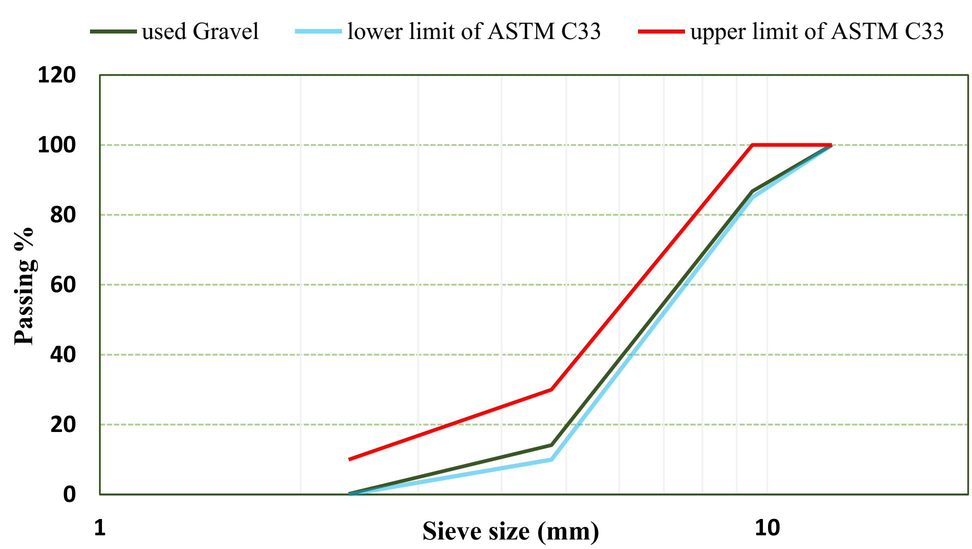

Fig. 2 Grading curve of normal weight coarse aggregate

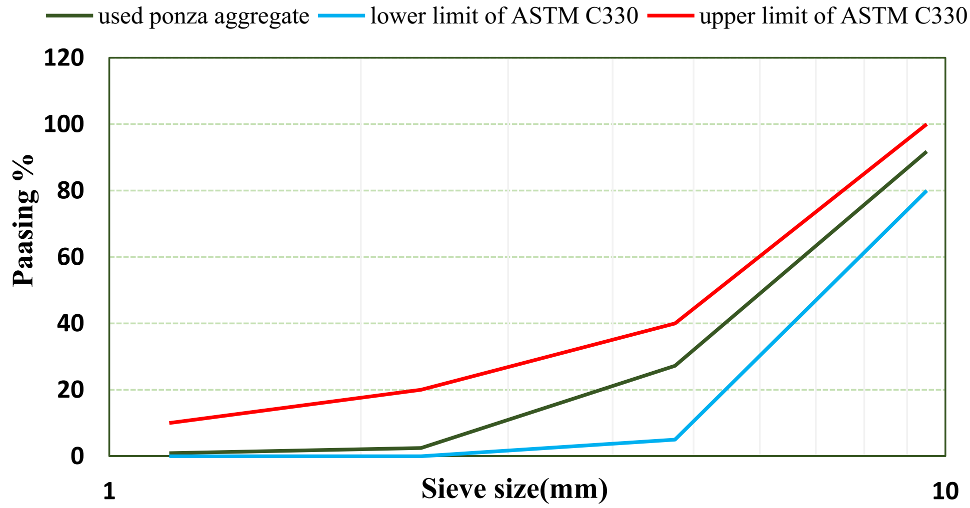

Fig. 3 Grading curve of light weight aggregate (Ponza)

Table 4 Physical properties of normal weight coarse aggregate

Property	Results
Specific gravity (SSD)	1.25
Water absorption%	41.6
Dry loose unit weigh (kg/m^3)	467
Dry rodded unit weight (kg/m^3)	489
Sulfate content SO_3	0.08
Fineness Modulus	5.7

to adjust the desired workability for all concrete mixes. It is free from chlorides and complies with ASTM C494-13 [36] type F. Table 5 shows the technical data obtained by the manufacture for this type of SP.

Recycled PET fibers: Reinforcing fibers in this work were constructed from waste PET bottles of crystal soft drink that were cleaned to remove impurities and formed into a segment. This segment was then cut by paper shredder into pieces of 4 mm wide along their length and a paper cutting machine was used to obtain the desired length in rectangular shape (Fig. 5). The tensile strength and modulus of elasticity for this type of recycled waste plastic fibers WPF (PET fibers) was 105 MPa and 0.57 GPa [37]. The physical properties of PET fiber used are given in Table 6.

Mixtures

Three different aspect ratios (length of the fiber/equivalent diameter) were selected in this investigation: 15, 30, and 45, and by equivalent diameter method the fiber lengths used were extracted as shown in example of aspect ratio = 15 below.

Example to determine desired length of WPF:

Fig. 4 spread out the light-weight aggregates to have SSD condition

Table 5 Technical data of superplasticizer

Appearance	Light brown / Turbid liquid
Density	1.084 ± 0.01
pH	4–4.8
Storage	Should be stored in original containers and at 5—35 °C
Transport	Not classified as dangerous

For aspect ratio = 15, calculate the equivalent diameter (d) by area equality:

width of PET fiber = 4 mm, thickness of PET fiber = 0.3 mm

$$\frac{\pi}{4}d^2 = widith * thikness$$

$3.14*d^2/4 = 4*0.3$

d = 1.234 mm.

l/d = 15.

l = 18.15 mm.

The estimated lengths for each aspect ratio are found in Table 7 whereas, Fig. 6 shows photographic views of these lengths of PET fiber.

Mix Proportion: Mixes in this investigation were carried out on two stages: in the first stage, the control mix of SCC named as MR was designed based on the guidelines of EFNARC [38] through preliminary experimentation using trial and error until the final proportions satisfied the SCC requirements. The best fresh and mechanical properties for

Table 6 physical properties of recycled PET fiber

Fiber color	Density (gm/cm^3)	Water absorption %	Aspect ratio(l/d)	Thickness (mm)	Width (mm)
crystal	1.37	0	15 30 45	0.3	4

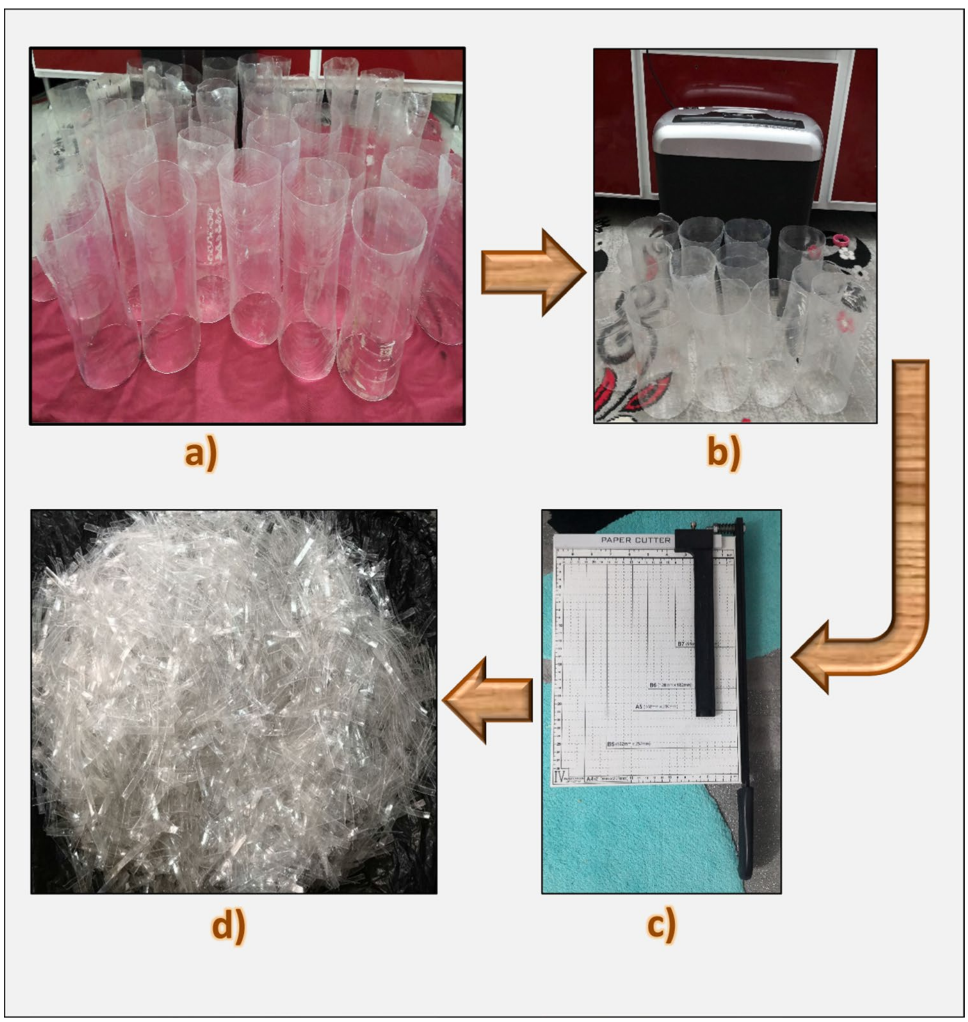

Fig. 5 Process used to form PET fibers **a** prepare soft drinks bottles. **b** paper shredder to cut bottle **c** paper cutting to obtain the desired length. **d** prepared fibers

Table 7 Length and dimension of all PET fiber used

Aspect ratio (l/d)	Length (mm)	Dimension (mm)
15	18.51	18.51 × 4 × 0.3
30	37.02	37.02 × 4 × 0.3
40	55.53	55.53 × 4 × 0.3

SCC were attained when the replacement level of fly ash as supplementary cementitious material was 20% and 40% by weight of cement [39]. Therefore, a total binder content of 500 kg/m^3 in all mixes of this study was acquired by incorporating 80% Portland cement and 20% fly ash by weight. The water/binder ratio and fine aggregates contents were kept constant in all mixes. To keep fresh properties in a desired range, SP dosage was adjusted at 2% by weight of binder. Then, another four mixes were obtained by substituting natural coarse aggregate (gravel) with lightweight coarse aggregates (Ponza) at different replacement ratios ranging from 40 to 100% at 20% increments by volume of natural aggregates in MR mix. The composition of the mixes in stage one is presented in Table 8.

Test results of mechanical properties for this mix have showed that the mix with 100% lightweight aggregate (M100) have lower splitting tensile strength and flexural strength, this result was in agreement with those obtained

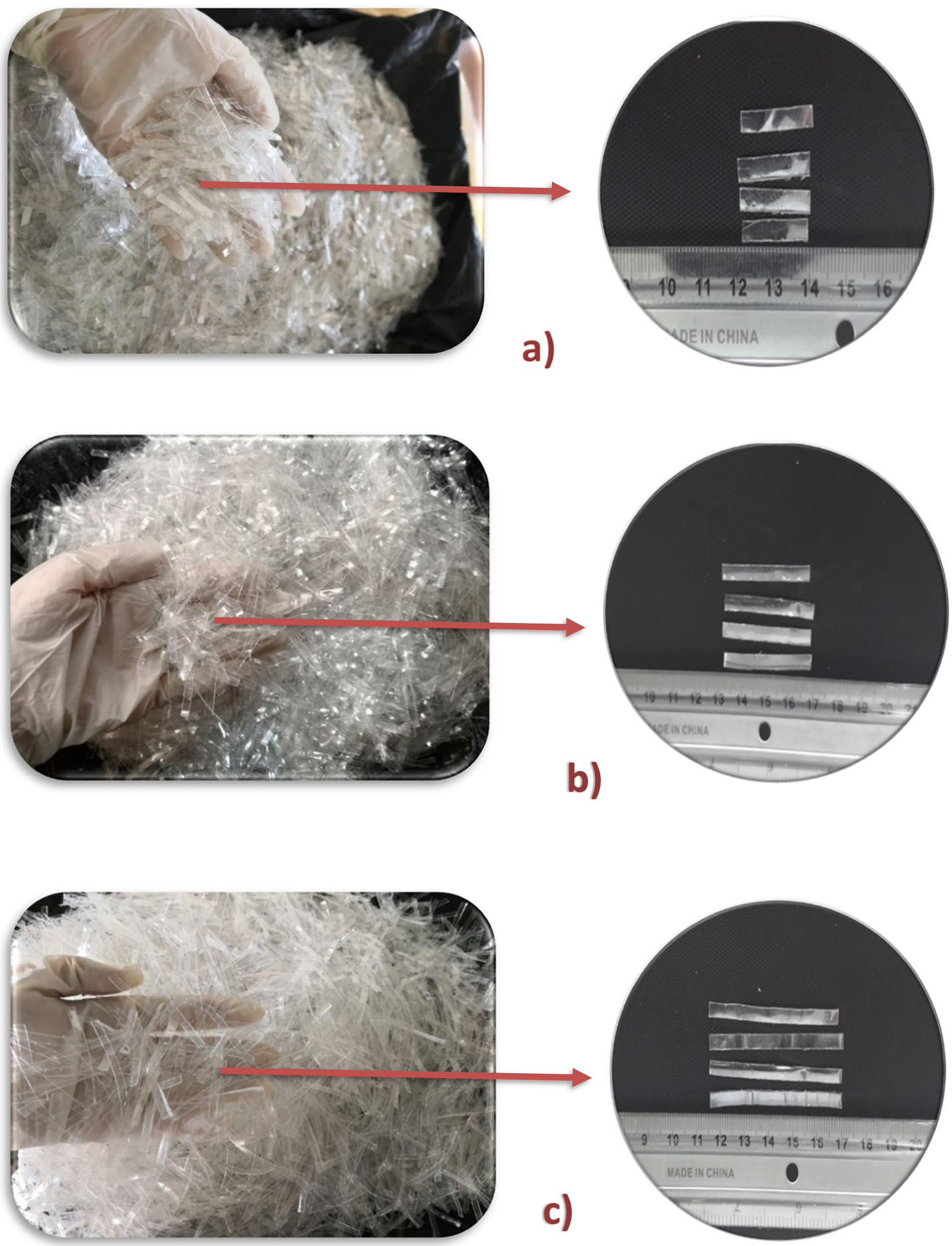

Fig. 6 Recycled PET fiber produced **a** length of 18.51 mm **b** length of 37.02 mm **c** length of 55.53 mm

Table 8 Concrete mix proportions in first stage

No	w/b	Binder content kg/m3		Natural aggregates kg/m3		Light weight aggregates kg/m3	Water kg/m3	HRWRA kg/m3
		Cement	Fly ash	coarse	fine			
MR	0.354	400	100	790	850	0	177	10
M40	0.354	400	100	474	850	149.2	177	10
M60	0.354	400	100	316	850	223.6	177	10
M80	0.354	400	100	158	850	298.11	177	10
M100	0.354	400	100	0	850	372.64	177	10

by Pannem and Kumar [40]. Thus, in the second stage the M100 mix was selected to be a control mix in order to enhance its ductility and tensile strength by adding fiber. Afterword, the weight proportion of all ingredient in M100 was reduced by the volumetric replacement of PET fiber using the relative specific gravities of each material. Three Aspect ratio (15, 30, and 45) and three volume fractions (0.5%, 0.75%, and 1%) of PET fiber were utilized to obtain another nine mixes in this stage as clearly appears from the mix proportions detailed in Table 8.

The abbreviation for the mixture name consists of two parts. The first part represents the volumetric percentage of plastic waste fibers (i.e., volume fraction aspect ratio). The second part represents the aspect ratio used in the concrete mix (i.e., the product of dividing the length of the fiber by its equivalent diameter), for example, F0.5%,15 means the presence of fibers in volume fraction of 0.5% and aspect ratio of 15.

Mixing procedure

The same mixing procedure was used in all concrete mixes to provide homogeneous and uniform mixture. Concrete mixing sequence started with mixing PET fiber with coarse and fine aggregate for one minute in a ban type mixer with capacity of 0.1 m^3. This was followed by incorporating cement and fly ash in the mixer and mixed until the dry ingredients become homogeneous. Then, the water containing HRWRA was added gradually to avoid segregation and the wet mixing continued for further 3 min. Finally, the concrete was left one minute for rest, and mixed again for one minute to obtain homogeneous mix.

Casting and curing

Immediately after the concrete mixing, Cubic, Cylindrical, prismatic, and slab specimens were cast in the prepared molds without any vibration. Before casting the concrete in molds, they were appropriately cleaned and lubricated with oil. Then, all these specimens were covered with nylon sheets. After 24 h of casting, the molds were demolded, and the specimens were cured in water tank.

Testing procedure

In this research, experimental investigations were conducted in three parts. In the first and second parts, investigations were performed on the fresh and hardened properties of concrete slabs, considering different mix proportions. In the third part, a detailed experimental study was conducted on the low velocity impact. Fresh-state tests for self-compacting slabs were performed within 15 min after the addition of the mixing water, based on standards and procedures of EFNARC guidelines [38]. The slump flow and T-500 tests were performed according to the EFNARC guidelines [38] in order to determine the followability of self-compacting concrete. In addition, L-box test was carried according to the EFNARC guidelines [38] out to check the passing abilities of fresh concrete. A sieve segregation test was performed to determine the segregation index (SI) [38].

Dry bulk density: In this investigation, it is crucial to acquire the dry bulk density of concrete after hardening, because the way to categorize the concrete as lightweight is to make sure that it matches the density criteria according to EN206 [9], which states that the concrete is lightweight when the oven-dry density is more than 800 kg/m^3 and not exceed 2000 kg/m^3. To find the dry bulk density, procedure explained in ASTM C567-14 [41] has been followed. **Compressive strength:** To measure the compressive strength development at ages of 7, 28, and 90 days, the test was conducted using three 100 mm cubes by testing machine (ELE-Digital) with 2000 kN capacity in terms of applying the load to the specimen continuously until failure. The test was carried out in accordance to the procedure outlined in BS EN 12390-3:2009 [42] standard. **Ultrasonic pulse velocity:** Measurements of ultrasonic pulse velocity on three 100 mm cubic specimens were conducted after 28 days of curing using equipment for generating ultrasonic pulse (type control italy) with frequency of 54 kHz and accuracy of 0.1, according to the ASTM C597-09 [43]. The acoustic impedance, defined by the pulse velocity and density (Eq. 1), is a measure of transmitting sound waves through medium [44].

$$Z = V_{\rho} \quad (1)$$

where
Z = acoustic impedance, kg/m^2 sec
V = ultra pulse velocity, $\frac{km}{s}$
ρ = density, kg/m^3

Thermal conductivity (k-value): The thermal conductivity tests were implemented on 100 mm cube at age of 28 days based on ASTM C 1113-90 (hot wire method) [45]. A measuring instrument (quick thermal conductivity meter QTM 500) equipped with a probe containing of thermocouple and heater wire, shown in Fig. 7. The principle of measuring k-value in QTM 500 as follow: a constant electrical energy is applied to a heater in probe, and the temperature of the hot wire will be increased. Then, linear curve is plotted between temperature and time scaled in logarithm. *k*-value is calculated using Fourier equation based on the slope of the curve and rate of temperature increase. This method, which determines the k-value by means of a transient method, takes a few minutes in contrast to the other methods including steady-state conditions. **Flexural toughness:** Toughness is a significant characteristic in concrete which demonstrates its resistance to failure under bending applied loads. It is the ratio of absorbed energy that can be determined as area under load—deflection curve. To measure the flexural toughness, four-point load test was performed using testing machine (type WDW- 200E) with loading rate of 0.075 mm/min on prismatic specimens with dimension of 100 × 100 × 400 mm at age of 28 days of curing, followed ASTM C 1609-12 [46]. The load was applied on a span length of 300 mm at 100 mm from both supports. The relationship between load and deflection is drawn by the software of testing machine as shown in Fig. 8.

Impact strength for concrete slabs: The test was conducted to compare the relative impact parameters of different volume fraction and aspect ratio of fiber in SCLC and to exhibit the enhanced performance of fiber-concrete compared to conventional concrete. A total of 20 slabs with dimension of 400 × 400 × 40 mm^3 were made for low velocity impact test, (see Fig. 9). The age of slabs was 90 days and average findings of two slabs was adopted. The apparatus used for this test consist of:

i. A steel tube (height of 2400 mm and diameter of 110 mm) used as vertical guide for falling ball to center the impact blow in the mid-span of the slab.
ii. Square support frame for supporting and fixing the concrete specimens. It was kept rigid by welding it to short columns separated from the testing machine in order to avoid any vibration that might affect the reading of the dial-gage (Fig. 9).

This test yields the number of blows caused by a steel ball of weight 1.4 kg and diameter of 55 mm that dropped freely without touching the tube from 810 mm height. A rubber strip of 40 mm width is used below the slaps to

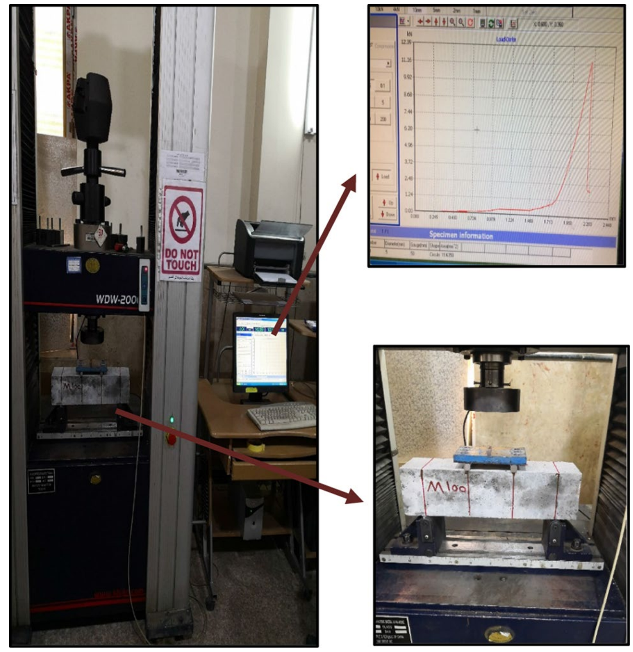

Fig. 8 Flexural toughness test

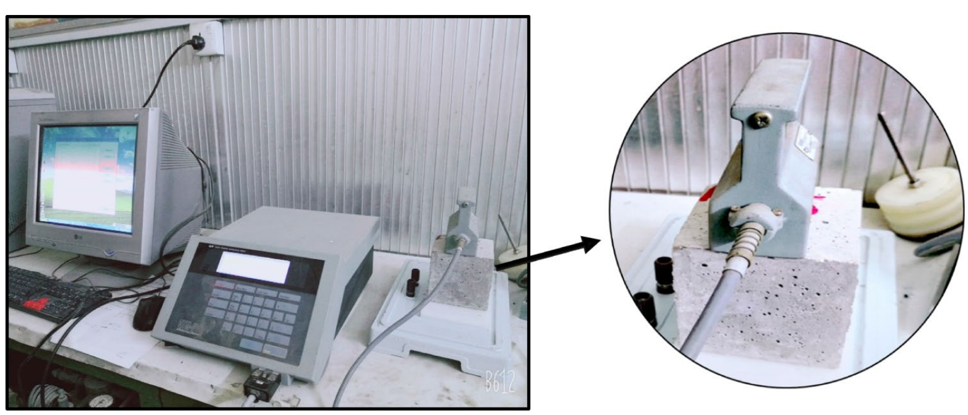

Fig. 7 The apparatus used to evaluate the thermal conductivity

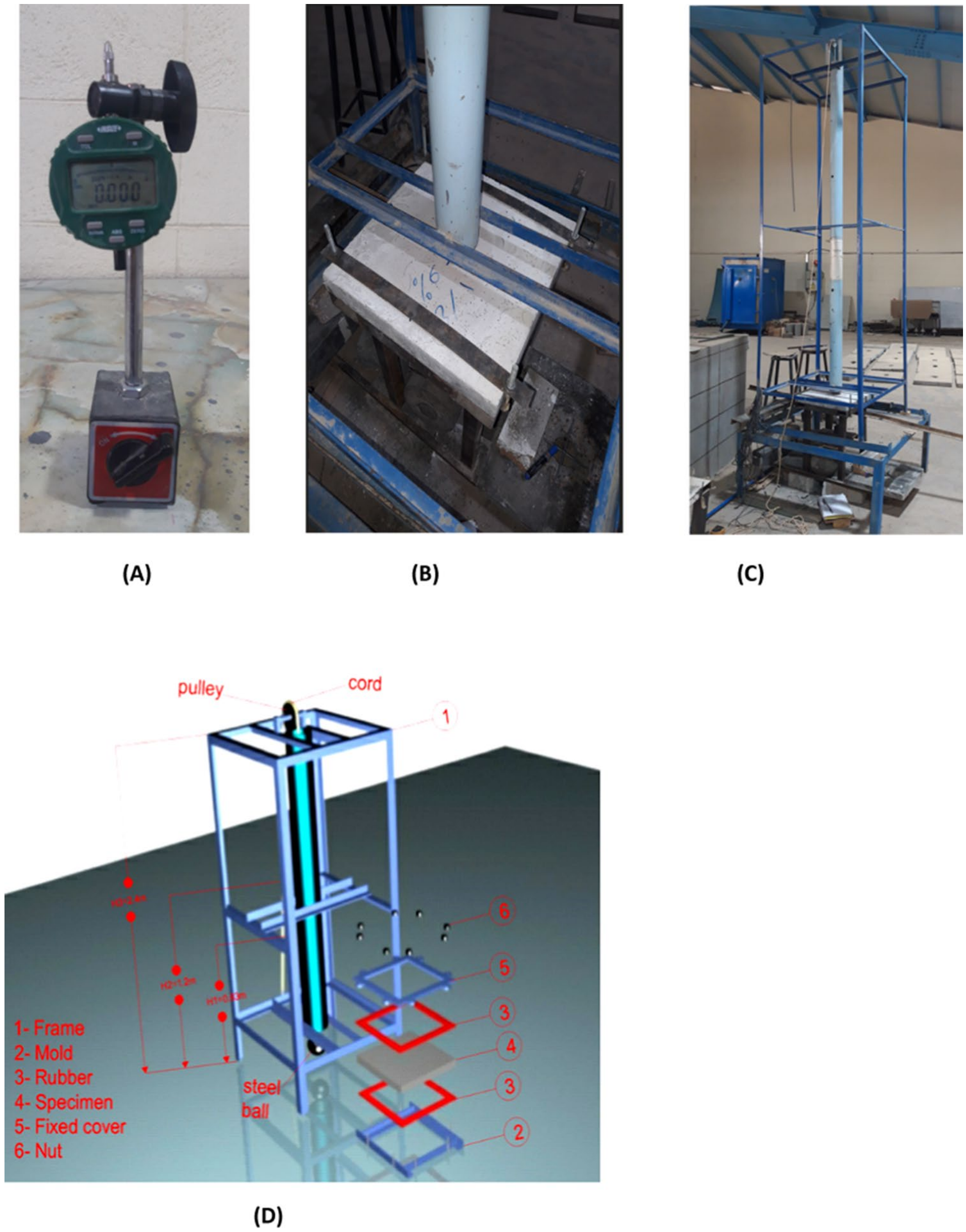

Fig. 9 **A** Digital gauge **B** Slab in impact testing machine. **C**: Impact testing machine. **D** Detailed diagram of the impact tester

reduce the effect of vibration. To compute the maximum deflection of slabs during the impact test, a special digital gauge, which can be locked at the maximum reading during the blows, is attached in the center below the concrete slabs as shown in Fig. 9. Three parameters called first failures, initial scabbing, and final failures, which testify the specimen resistance to impact load, were noted. First failure represents the number of blows caused the first visible crack in slab specimen, initial scabbing represents the number of blows caused first scabbing in the distal face, and final failure represents the number of blows caused no response by specimen to impact load. The impact energy was determined using Eq. (2) [47].

$$\mathrm{EI} = \mathrm{N} \times \mathrm{m} \times \mathrm{g} \times \mathrm{h} \tag{2}$$

where
EI = Energy of impact, N m
N = number of blows
m = mass of the dropping hammer, kg
g = gravity acceleration, m/s^2
h = height of drop hammer,

Results and discussion

Increasing the slump flow diameter and L-box height ratio, respectively, simultaneously improved the filling and passing capacity. This was discovered when the replacement level of lightweight aggregate was increased. According to the EFNARC guidance, all of the mixes demonstrated high resistance to segregation despite the increase in the segregation index brought on by the inclusion of lightweight aggregate. With the exception of the mix containing only 100% lightweight aggregates, all mixes had compressive strengths more than 42 MPa at 28 days of SCLC.

Dry bulk density

The mixtures' dry bulk densities have been measured, and Fig. 10 compares the densities for the MR, M40, M60, M80, and M100 mixtures. Compared to SCC's dry density of 2305 kg/m^3, SCLC's dry density ranges between 1703 and 2040 kg/m^3. It was observed that a decrease in dry density resulted from an increase in the volumetric replacement of lightweight aggregate. For instance, the dry density of the M40, M60, M80, and M100 mixes, when compared to the MR mix, was as low as 11.5%, 16.5%, 21.08%, and 26.1%, respectively. Ponza aggregates' low weight might be responsible for the reduction in the weight of concrete. In conclusion, replacing Ponza aggregates would result in a roughly 12–26% reduction in the dead load of structural buildings. The change in dry density of all mixes in the second stage mixes are graphically exemplified in Fig. 11. As observed in this Figure, the control mix M100 has the highest dry density followed by series of mixes with PET fiber of 0.5%, 0.75%, and 1%, sequentially. At same aspect ratio of 30 and compared to M100 mix, dry density decreased by 2.8%, 4.5%, and 6% for mixes with 0.5%, 0.75%, and 1% fibers, respectively. Generally, the addition of PET fibers in SCLC mixture decreases the dry density of the mixture. Furthermore, results of dry density in the mixes containing longer fibers (aspect ratio of 45) gives lower densities, regardless of the fiber content. This may be because utilizing long fibers at a high ratio leads to increased voids in concrete caused by the fibers' balling impact and incomplete consolidation. [48].

Ultrasonic pulse velocity

The UPV experiment is conducted for the estimation the quality of concrete, as well as it is a good indication about the presence of internal voids and cracks. The effect of lightweight aggregates as a volumetric replacement of natural aggregates on UPV of SCC is presented in Fig. 12. This Figure clearly shows that the UPV of concretes decreased noticeably depending on the amount of lightweight particles used. The SCC mixtures with 100% natural aggregate (MR) showed the maximum pulse velocity value, whereas the mixture with 100% lightweight aggregate (M100) showed the lowest pulse velocity. The UPV of mixes containing 40%, 60%, 80%, and 100% lightweight particles was specifically 2.8%, 7.8%, 9.7%, and 13% lower than that of the control concrete, respectively. The use of lightweight aggregate has a substantial impact on dropping density and rising voids, which leads to decreased UPV, according to the findings of bulk density and porosity tests. All the produced SCC and SCLC in this stage had velocity values above 4 km/sec, so the concretes were considered to be good and excellent of quality [49]. Figure 13 compares the UPV of SCLC at different ratios and lengths of PET fiber. It was observed, as predicted, that the UPV values marginally dropped as the

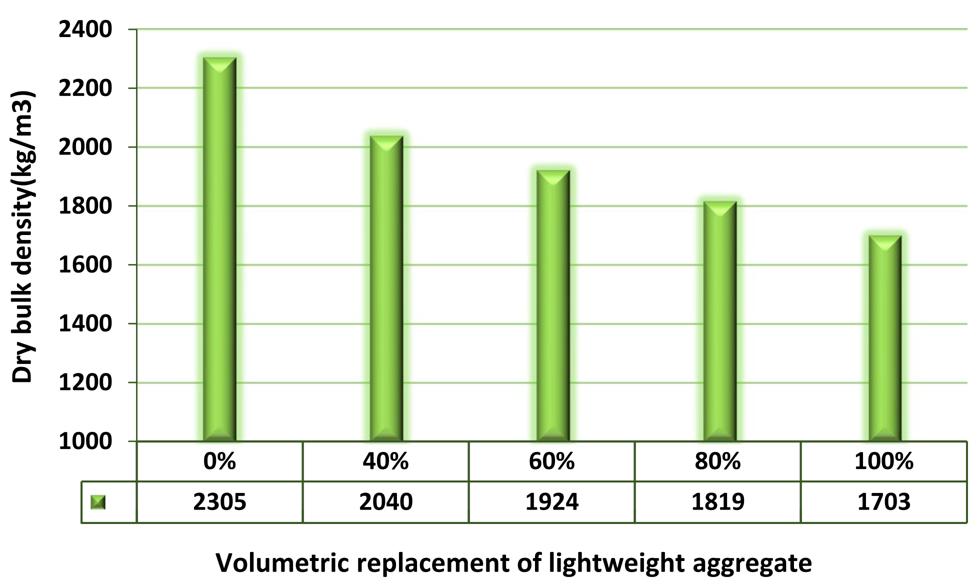

Fig. 10 Effect of lightweight aggregate on dry bulk density of hardened SCC

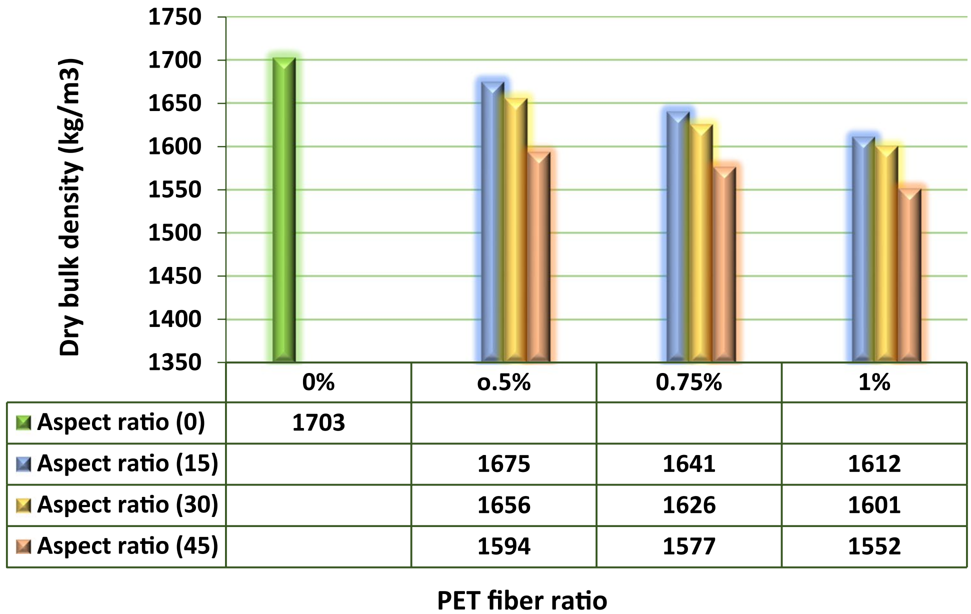

Fig. 11 Effect of PET fibers on dry bulk density of hardened SCLC

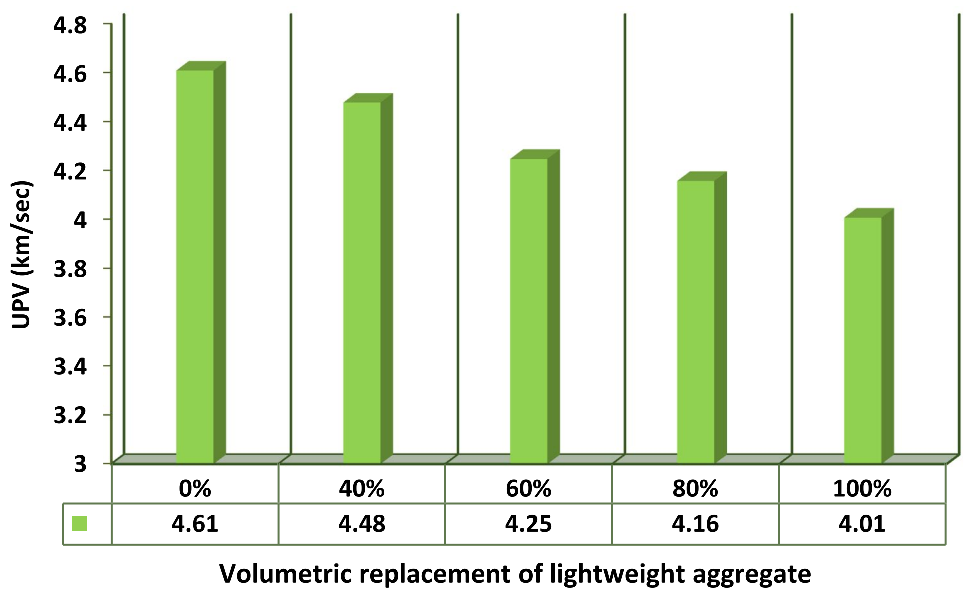

Fig. 12 Effect of lightweight aggregates on UPV

volume % of PET fiber increased. However, where this test is not spastically developed for fiber reinforced concrete, the inclusion of PET fibers may significantly change the velocity values. The reduction in the UPV of the SCLC with 0.5%, 0.75%, and 1% at the same aspect ratio of 15 were 1.7%, 4.4%, and 8.2%, respectively, compared to the control concrete. The cause is that PET fiber's balling during tamping may actually contribute to increasing the voids. Additionally, adding fiber and using PET fiber with a larger aspect ratio had a negative impact on the concrete specimens' pulse velocities. For instant, the mix with 0.5% and aspect ratio of 15 had a UPV of 3.94 km/sec, while in F 0.5% 30 and F0.5% 45 the UPV were 3.87 and 3.65 km/sec, respectively. The UPV values for all second stage mixes at age 28 days ranged between 3.47 and 4.01 km/ sec. According to these values, SCLC with PET fiber prepared in this study can be categorized as a good quality concrete [49].

Acoustic impedance

The acoustic impedance is carried out in this investigation to assess the loudness in concrete at different ratio of lightweight aggregates and different volume fraction of PET fiber (Table 9). The acoustic impedance, defined by

Fig. 13 Effect of PET fiber on the UPV

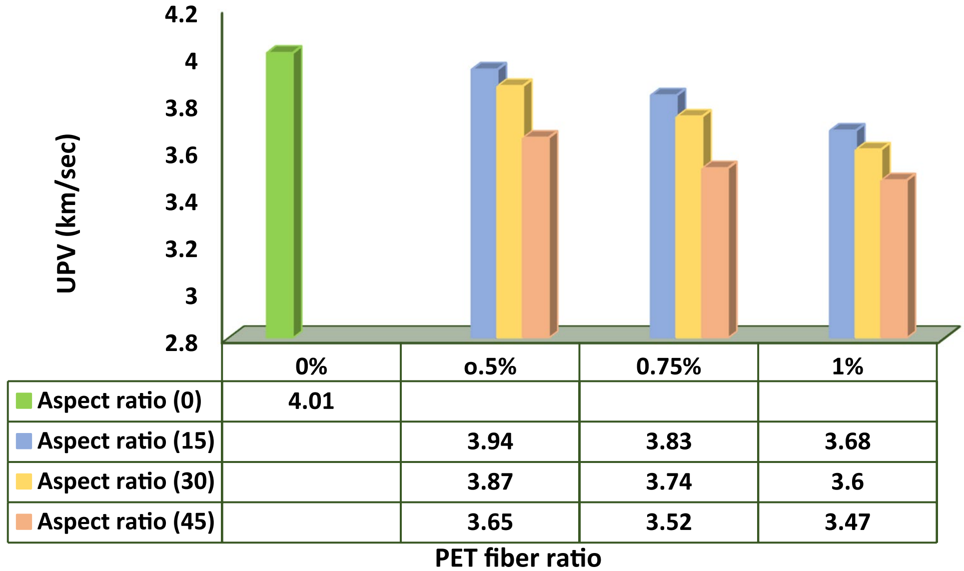

Table 9 Concrete mix proportions in kg/m^3 (second stage)

NO	Water	Cement	Fly ash	Fine aggregate	Lightweight aggregate	HRWRA	PET fiber
M100	177	400	100	850	372.6	10	0
F0.5%,15	176.1	398	99.5	845.8	370.8	9.95	6.85
F0.75%,15	175.7	397	99.25	843.6	369.8	9.925	10.27
F1%, 15	175.2	396	99	841.5	368.9	9.9	13.7
F0.5%,30	176.1	398	99.5	845.8	370.8	9.95	6.85
F0.75%,30	175.7	397	99.25	843.6	369.8	9.925	10.27
F1%,30	175.2	396	99	841.5	368.9	9.9	13.7
F0.5%,45	176.1	398	99.5	845.8	370.8	9.95	6.85
F0.75%,45	175.7	397	99.25	843.6	369.8	9.925	10.27
F 1%,45	175.2	396	99	841.5	368.9	9.9	13.7

the pulse velocity and density, is a measure of transmitting sound waves through medium [50].

$$Z = \rho V \quad (3)$$

where
Z = acoustic impedance, kg/m^2 sec
V = ultra pulse velocity, $\frac{km}{s}$
ρ = density, kg/m^3

Tables 10 and 11 show the effect of lightweight aggregate and PET fiber on the acoustic impedance, respectively. From Table 10, it can be observed that increase in substitution level of lightweight aggregate causes a reduction in acoustic impedance value. For instance, group concretes with lightweight particles (M40, M60, M80, and M100 mixes) had an approximate 14–36% lower acoustic impedance than MR mix. As a result, utilizing concrete containing Ponza aggregates instead of natural aggregates could boost sound insulation in structural members by 36%.

Table 10 Effect of lightweight aggregates on the acoustic impedance

Mix code	Ultrasonic pulse velocity (km/sec)	Density (kg/m^3)	Acoustic Imped-ance $\times 10^6$ (kg/m^2.sec)
MR	4.61	2305	10.63
M40	4.48	2040	9.14
M60	4.25	1924	8.18
M80	4.16	1819	7.56
M100	4.01	1703	6.83

Table 11, which summarizes this information, shows that using PET waste as fiber also helps to reduce the acoustic impedance of SCLC by roughly 21%. This is

Table 11 Effect of PET fiber on the acoustic impedance

Mix code	Volume fraction of fiber(%)	Aspect ratio of fiber	Ultra pulse Velocity(km/sec)	Density (kg/m^3)	Acoustic Impedance $\times 10^6$ (kg/m^2.sec)
M100	0	0	4.01	1703	6.83
F0.5% 15	0.5	15	3.94	1675	6.59
F0.5% 30		30	3.87	1656	6.4
F0.5% 45		45	3.65	1594	5.81
F0.75% 15	0.75	15	3.83	1641	6.28
F0.75% 30		30	3.74	1626	6.08
F0.75% 45		45	3.52	1577	5.55
F1% 15	1	15	3.68	1612	5.93
F1% 30		30	3.6	1601	5.76
F1% 45		45	3.47	1552	5.38

probably because blends containing PET fiber have gaps, which enhance sound insulation.

Thermal conductivity

The typical measurement of thermal conductivity values for mixes in the first stage are presented in Fig. 14. When lightweight aggregate content was taken into account, it was concluded that as the replacement level of lightweight aggregates increased, thermal conductivity decreased. It is clear from Fig. 14 that the highest thermal conductivity was in control concrete MR, while the lowest value was in M100 mix. In other words, with respect to MR mix the decrease in thermal conductivities were 18.5%, 31.4%, 34.3%, and 46.1% for M40, M60, M80, and M100 mixes, respectively. The use of Ponza aggregate, which has highly porous structure, as a substitute of gravel aggregates is a consequence of the increase in the voids (porosity) and the decrease in density and hence, thermal conductivity drops. This result is confirmed by Penelope and Williams [46] and ACI committee [47] for another type of lightweight aggregate.

Figure 15 shows graphically the relationship between the ratio of PET fibers and heat conductivity at various fiber aspect ratios. It can be seen that the SCLC's thermal conductivity somewhat decreases when the ratio of PET fibers increases.

Control concrete M100 with no fiber content had a thermal conductivity of 0.96 W/Mk, while concrete with 0.5%, 0.75%, and 1% PET fiber contents had values of 0.82, 0.81, and 0.78 W/mK, respectively. With PET fiber levels of 0.5%, 0.75%, and 1%, respectively, at the same aspect ratio of 45, there is therefore a nearly 14.6%, 15.6%, and 18.7% reduction in thermal conductivity. It is evident also that with the increase length of PET fiber, there is decrease in thermal conductivity of the SCLC mixes. Values show that for same fiber ratio of 0.75% there was around 7% decline in thermal

Fig. 14 Effect of lightweight aggregates on the thermal conductivity

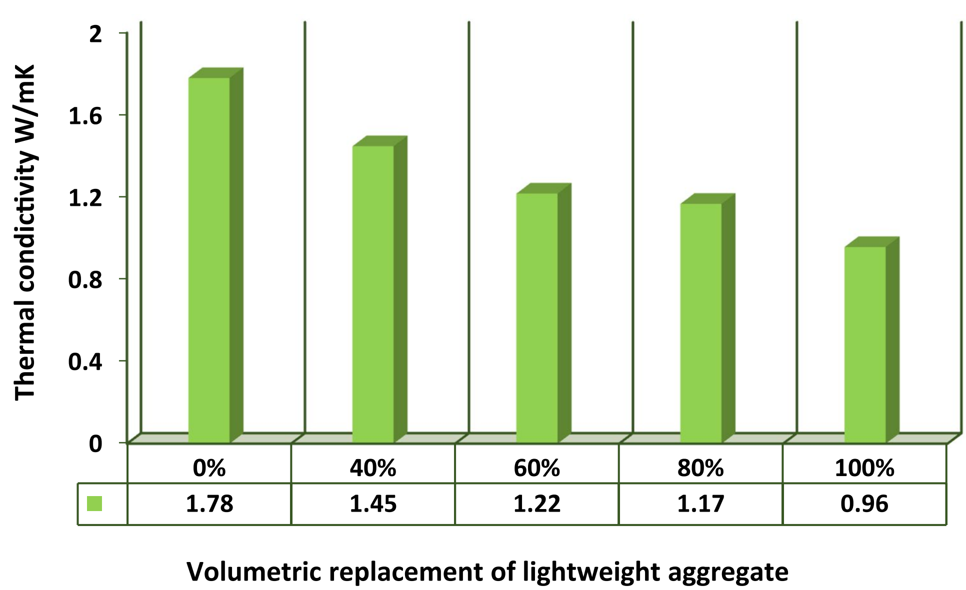

Fig. 15 Effect of PET fiber on the thermal conductivity

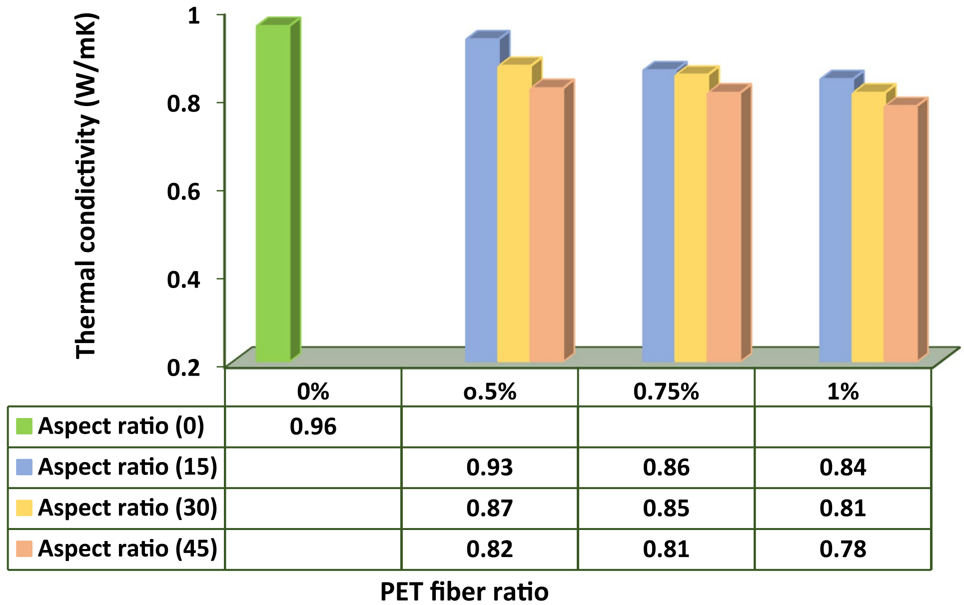

conductivity with increase in fiber aspect ratio from 15 to 45. This reduction in the value of thermal conductivity is associated to increase pore structures in concrete when incorporation PET fiber.

The conclusion is certified not only out own results, but also other studies [51, 52]. As a summary, both lightweight aggregates and PET fiber have reduced thermal conductivity and this contributes to an enhancement in heat insulation and achieving optimized condition in concrete against the effect of fire. This might make this type of concrete more efficient to be used to reduce the cost of heating and cooling of concrete buildings in summer and winter, respectively. Thermal conductivity depends upon the density of concrete. So, Topçu et al. [53] has proposed a relationship between *K*-value and dry unit weight (ρ) as follow [53]:

$$K = 0.0864e^{0.00125\rho} \tag{4}$$

In this investigation, the relationship between *K*-value and dry bulk density regardless the effect of lightweight aggregates and PET fiber was plotted in Fig. 16. The results in this Figure show that the thermal conductivity of SCLC produced with lightweight aggregate and WPF can be predicted from its dry bulk density using Eq. (5) [53].

$$\mathrm{K} = 0.131e^{0.0012\rho} \tag{5}$$

There is a slight difference between both equations. This can be due to the fact that the SCC is distinguished from the ordinary concrete by the abundance of fine materials, which works to reduce porosity and thus increase the coefficient of thermal conductivity.

Fig. 16 Relationship between thermal conductivity and dry density

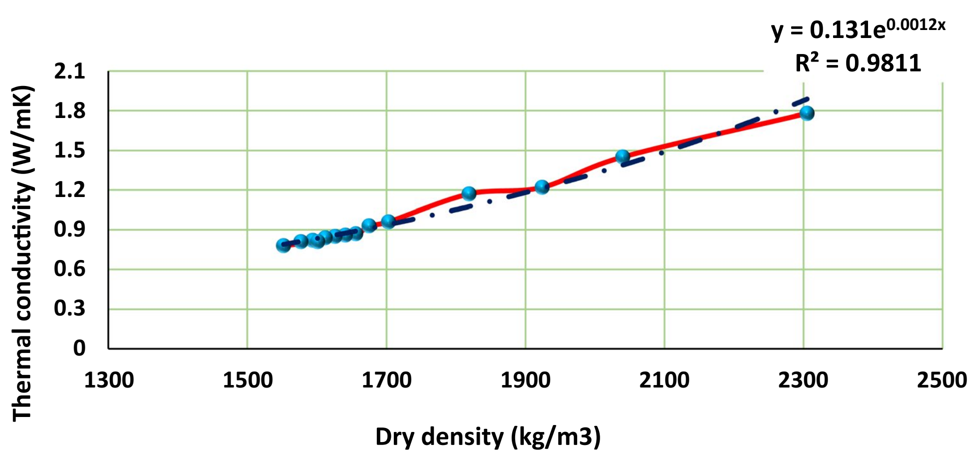

Flexural toughness

As known from the previous literature, the significant influence of fiber on concrete is to improve post- peak behavior. Thus, flexural toughness is an essential parameter to assess this influence.

Many methods have been suggested to achieve flexural toughness. The ASTM C 1906 method was used in this investigation to calculate flexural toughness [46]. Load–deflection curves for the SCLC and SCLC with PET fiber mixes are displayed in Figs. 17, 18, 19, 20, 21, 22, 23, 24, 25, 26.

The result based on the mentioned figures indicated that the maximum load of control specimen lower than maximum load of the specimens with PET fiber. Also, the response in the post-cracking region differentiated in specimen without fiber (control) from specimens with PET fiber. Control specimen behavior was a sudden drop in load–deflection curve once the peak-point of loading was reached. Thus, this specimen failed in a brittle mode

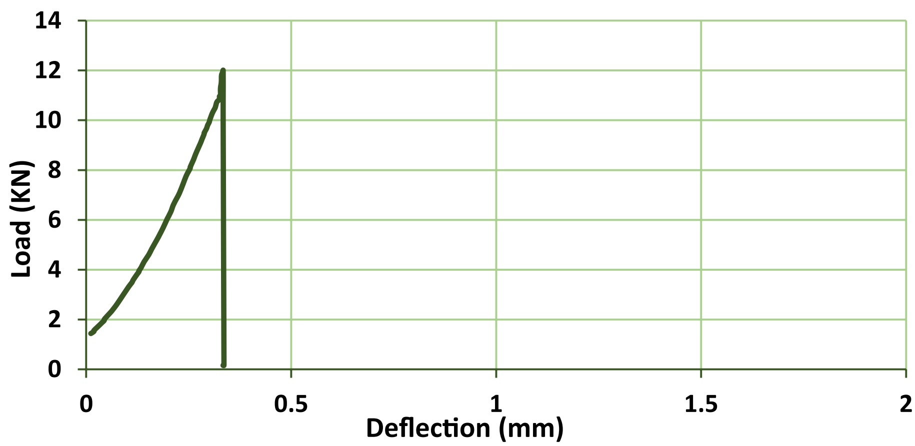

Fig. 17 Load–deflection curve for M100 mix

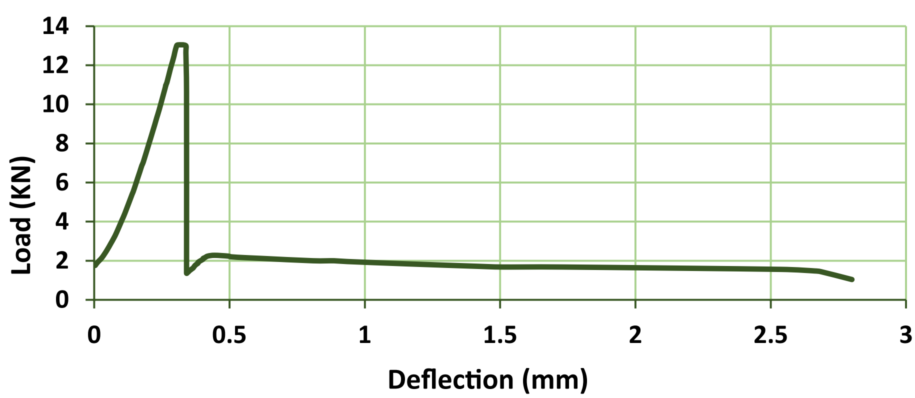

Fig. 18 Load–deflection curve for F 0.5% 15 mix

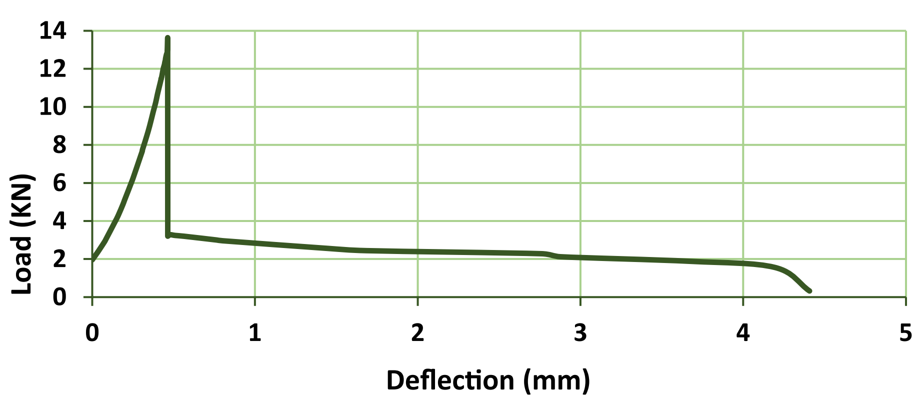

Fig. 19 Load–deflection curve for F 0.5% 30 mix

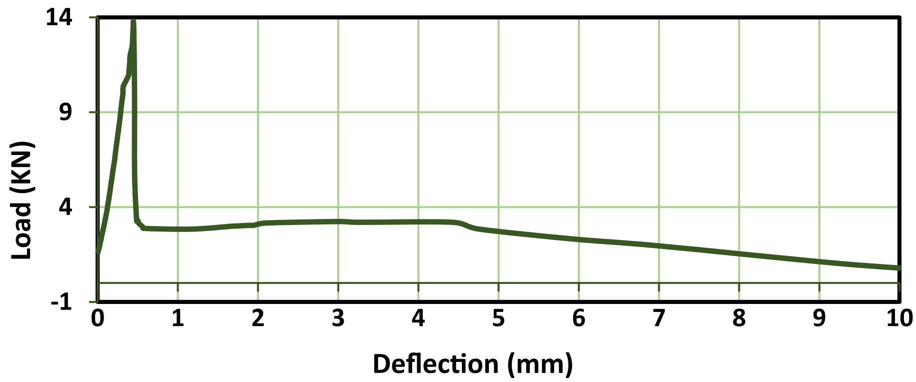

Fig. 20 Load–deflection curve for F 0.5% 45 mix

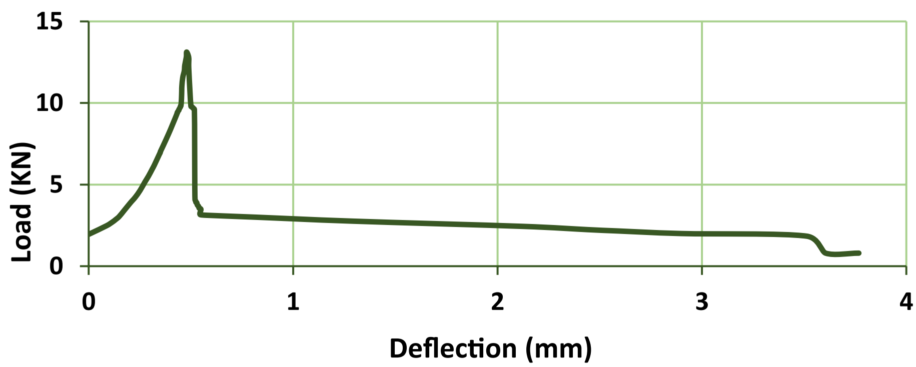

Fig. 21 Load–deflection curve for F 0.75% 15 mix

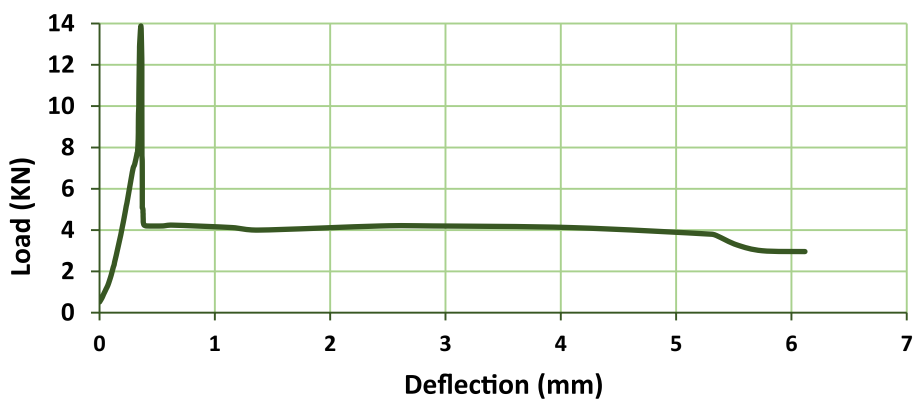

Fig. 22 Load–deflection curve for F0.75% 30 mix

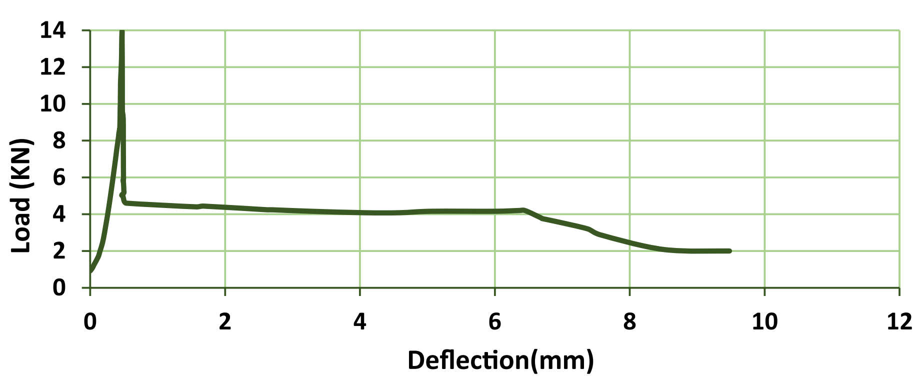

Fig. 23 Load–deflection curve for F 0.75% 45 mix

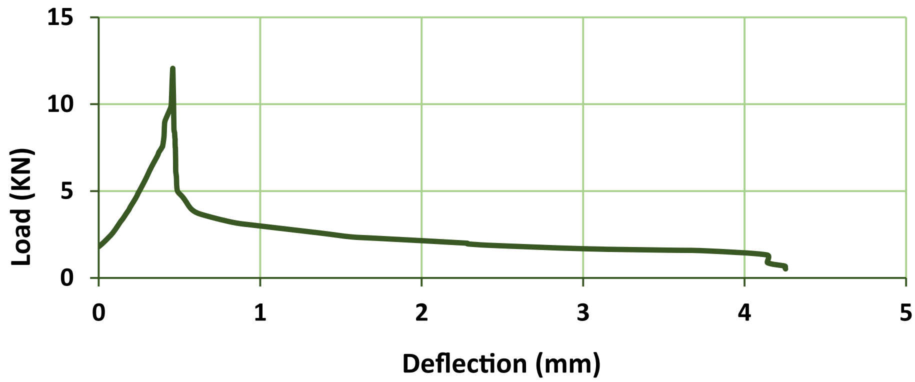

Fig. 24 Load–deflection curve for F 1% 15 mix

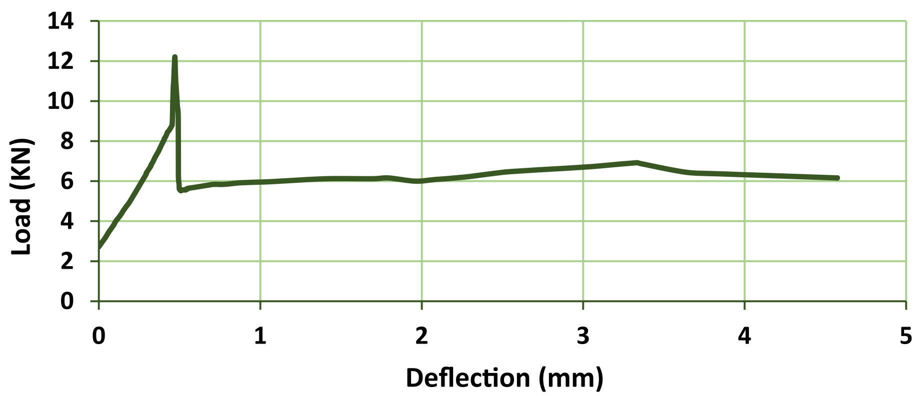

Fig. 25 Load–deflection curve for F 1% 30 mix

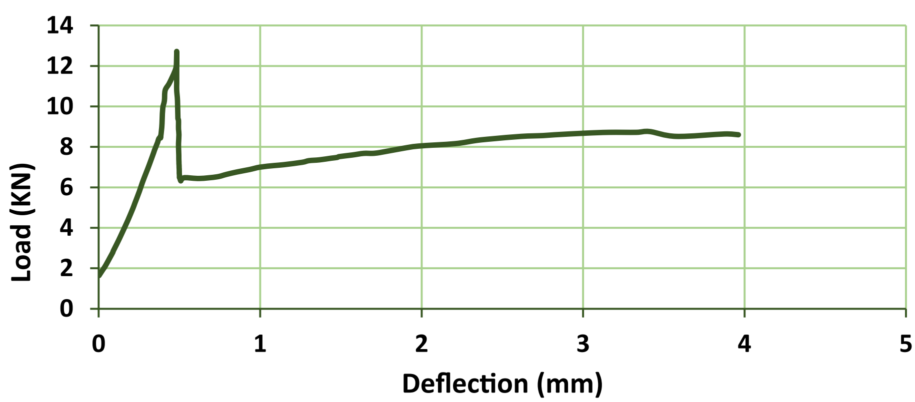

Fig. 26 Load–deflection curve for F 1% 45 mix

and separated into two pieces, while specimens with fibers exhibited a ductile behavior due to bridging effect of fiber that carry load after the peak. The work of plastic fibers begins after the first crack. It represents the highest load on the load–deflection curve. The fibers will redistribute the stresses and transfer them to the matrix on both sides of the crack. After that, the load will gradually decrease at increase deflection until the final failure occurs. Therefore, the behavior of strain softening could be seen in concretes containing PET fibers. Also, the area under load–deflection curve increased as volume fraction of fiber increased which states the enhancement of flexural toughness. The toughness is assessed by calculation the area under the load–deflection curves from net deflection zero up to span length /150 according to ASTM C 1609-12. Another parameter such as peak first load and residual strength at two deflections (L/600 and L/150) were determined as illustrated in Table 12 and the definition of these parameters are shown in Fig. 27.

As shown in Table 12, the incorporation of PET fibers had slightly affected the load of first crack. Compared to control concrete M100, there is an increase in first crack load of SCLC in range of 8.6%- 16.3% with the increase in PET fiber content up to 0.75% [7, 54].

Table 12 Results of flexural toughness and residual strength of mixes

Mix code	Pp (KN)	fp (MPa)	$P\frac{D}{600}$(KN)	$f\frac{D}{600}$ (MPa)	$P\frac{D}{150}$ (KN)	$f\frac{D}{150}(MPa)$	$T\frac{d}{150}$
M100	12	3.6	–	–	–	–	–
F0.5% 15	13.04	3.91	2.24	0.67	1.7	0.51	5.535
F0.5% 30	13.64	4.09	3.2	0.96	2.4	0.72	7.259
F0.5% 45	13.8	4.14	3.25	0.98	3	0.9	8.174
F 0.75% 15	13.12	3.94	2.92	0.88	2.44	0.73	7.392
F0.75% 30	13.88	4.16	4.31	1.29	4.18	1.25	8.424
F0.75% 45	13.96	4.19	4.62	1.39	4.42	1.32	9.08
F1% 15	12.04	3.62	4.68	1.4	2.38	0.72	7.422
F1%30	12.2	3.66	5.56	1.67	6.08	1.83	12.464
F1% 45	12.72	3.82	6.32	1.89	8.16	2.45	15.572

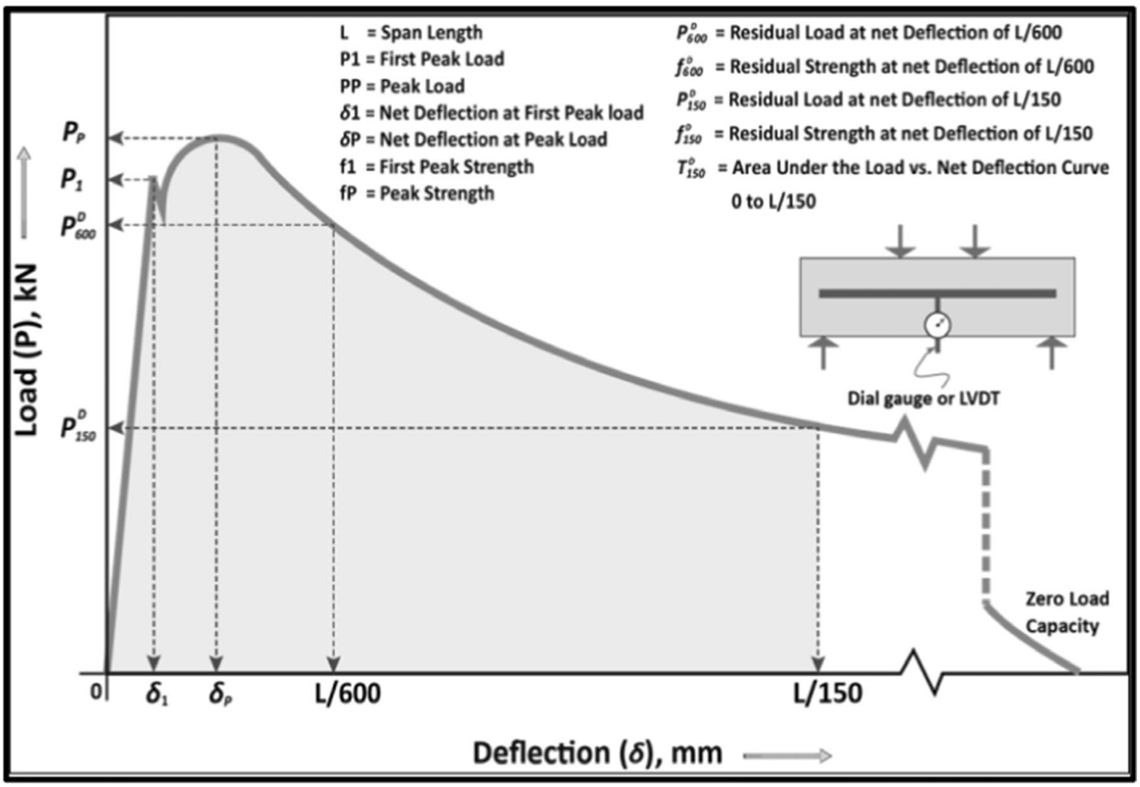

Fig. 27 Definition of parameters according to ASTM C1609-12

On the other hand, there was a significant positive influence for fiber on the post-cracking behavior. The area under curve ($T\frac{D}{150}$) of all SCLC increased with addition PET fiber in the SCLC. The highest amount of $T\frac{D}{150}$ is achieved by F 1% 45 specimen. On average, this value was 15.5726 KN.mm and it is almost 181.4% higher than the one with F0.5% 15. Also in this case, the residual strength increased proportionally to the content of PET fiber added to the SCLC. The residual strength value of D/150 standing at 0.51 MPa for F 0.5% 15 mix increased to 2.45 MPa for F1% 45 mix. It is clearly, that the toughness (energy absorption capacity) and residual strength of the SCLC was greatly improved with higher aspect ratio of fiber. The present finding indicated in line pattern with results of Faisal et al. [55].

Borg et al. [56] found that increasing volume fraction of recycled PET fiber provided better toughness and residual strengths of concrete.

Impact strength of concrete slabs

The impact slabs test responses include the number of impacts that result in the first crack, the initial scabbing, and the perforation (final failure). The energy that the SCLC slabs absorbed when struck was then calculated. For investigation of the impact behavior, the maximum displacements in the first crack at the middle of the bottom of the slab were also recorded. Based on the image processing technique, additional impact test characteristics such as mode failure and fracture pattern were reported.

Number of impact blows and energy absorption

Number of blows and energy absorption to first crack, initial scabbing, and perforation are summarized in Tables 13 and 14. From Table 13, it can be concluded that, the concrete slabs without plastic waste fibers had a lower number of blows that caused the appearance of the first crack as compared to those with plastic waste fibers. It can also be noted that the increase in the volumetric fiber ratio has a positive effect on the number of blows that cause the first crack and final failure.

After the initial crack, the SCLC slab exhibited brittle behavior and had the lowest impact resistance. The SCLC slabs containing fiber, however, could withstand more blows up until the perforation. The specimen of control concrete had the poorest overall impact resistance of all the test specimens. The increase in the impact resistance at post-cracking reign is depending on the content and aspect ratio of PET fiber. The increases in number of blows at ultimate failure over the corresponding control concrete mix were almost 206.6%, 320%, and 373.3%, respectively, through the addition of PET fibers at volume fraction of 0.5%, 0.75%, and 1% with similar aspect ratio of 45. Furthermore, SCLC with short fiber showed lower impact resistance than with long one due to low fiber-matrix bond strength (e.g., the number of blows to cause first and ultimate failure for F 1% 15 was 2 and 54, respectively, while it was 3 and 71 for F 1% 45).

With increasing PET fiber content and length, variations in impact results also arise in the initial scabbing blow count. Similar to how the first scabbing in M100 showed in the third impact blow, but not in F1% 45 until 22 blows later. According to that, a significant improvement in impact resistance is basically accomplished by using PET fiber in structural SCLC. Table 13 clearly shows that MI00 concrete have the lowest energy absorption capacity. For instance, energy absorption was found to be 11.12, 33.37, and 166.87 Joules for M100 concrete as well as 33.37, 244.74, and 789.84 Joules for F1% 45 concrete at first crack, initial scabbing, and ultimate failure, respectively. However, SCLC with WPF had increased 127–373% in energy absorption at ultimate failure with respect to control concrete. Thus, the addition of PET fiber enables SCLC to absorb more impact energy in comparison with plain concrete. The reason behind improvement of impact resistance and energy absorption may be attributed to high ductility capacity of concrete reinforced with WPF, which resist the propagation of cracks by bridging it and delay the occurrence of whole collapse of concrete slab. The impact results are consistent with previous findings [26, 27].

Figure 28 presents the results of the measured maximum central deflection at the first crack for different volumetric

Table 13 Number of impact blows at first crack, initial scabbing, and ultimate failure

Mix code	Volume fraction of fiber(%)	Aspect ratio of fiber	Number of blows to cause		
			First crack	Initial scabbing	Ultimate failure
M100	0	0	1	3	15
F0.5% 15	0.5	15	1	8	34
F0.5% 30		30	2	9	41
F0.5% 45		45	2	13	46
F0.75% 15	0.75	15	2	11	43
F0.75% 30		30	3	15	55
F0.75% 45		45	3	16	63
F1% 15	1	15	2	14	54
F1% 30		30	3	21	66
F1% 45		45	3	22	71

Table 14 Energy absorption at first crack, initial scabbing, and ultimate failure

Mix code	Volume fraction of fiber (%)	Aspect ratio of fiber	Energy absorption at		
			First crack	Initial scabbing	Ultimate failure
M100	0	0	11.12	33.37	166.87
F0.5% 15	0.5	15	11.12	89	378.23
F0.5% 30		30	22.25	100.12	456.11
F0.5% 45		45	22.25	144.92	511.73
F0.75% 15	0.75	15	33.37	122.37	478.36
F0.75% 30		30	33.37	166.87	611.85
F0.75% 45		45	33.37	178	700.85
F1% 15	1	15	22.25	155.74	600.73
F1% 30		30	33.37	233.61	734.22
F1% 45		45	33.37	244.74	789.84

Fig. 28 Max. deflection at first crack

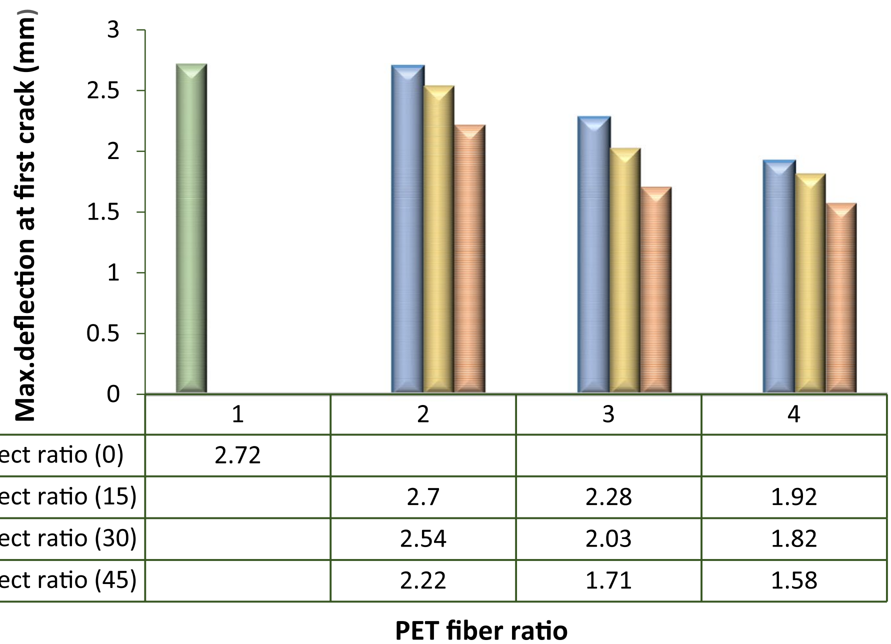

ratio and aspect ratio of WPFs for all concrete slabs. Under impacts from the similar drop height, the reference concrete specimens underwent larger deflections in comparison with the specimens reinforced with WPF. The maximum deflection measured by the digital gage decrease by about 42% due to the PET fibers effect.

Failure and crack patterns

The majority of the cracks on the top and distal face of the slab radiate outward from the impact site (the middle of the slab) and were concentrated along the diagonals. In essence, the hairline was the first crack on every specimen. More impact hits caused more recent cracks to form along the center axis. Then, new fissures appeared on the surface and old ones grew wider. According to Fig. 29 failure mechanism, control concrete specimens showed brittle shear failure in which fragments detached and broke the specimen into pieces, whereas WPF-reinforced specimens showed localized failure at the impact point and no fragments detached because the PET fiber helped hold the various fragments together. In addition, reinforced specimens exhibited more ductile failure process than the plain specimen and smaller deformation prior to complete perforation. Generally, incorporation of PET fiber in SCLC significantly improved resistance of impact and reduced damage. For M100 concrete, typical scabbing on the tension surface appeared on third blow but in reinforced slabs more blows required to cause serious scabbing on tension surface and cracking occurring much later in comparison with the M100 concrete. Also, number and width crack at ultimate failure decreased with increase content of PET fibers (Fig. 30). About three hairline cracks were found on reinforced slab specimen of 1% volume fraction and 45 aspect ratio of WPFs. Larger amount of cracks was noticed for other specimens.

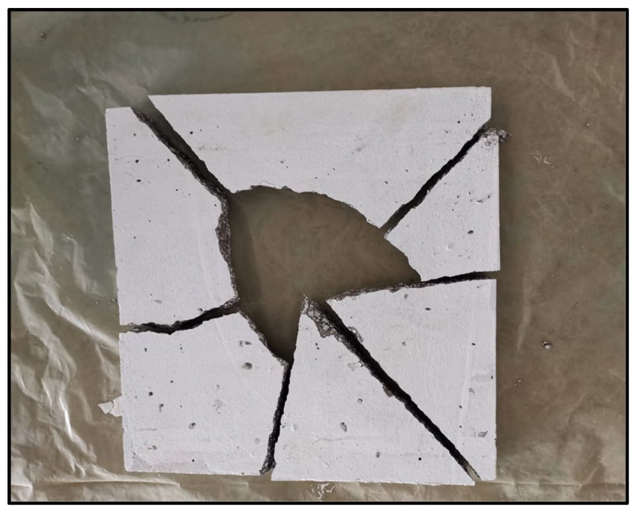

Fig. 29 Failure Pattern of control specimen

Conclusions

The obtained experimental results show that self-compacting lightweight concrete with dry density of 1700 kg/m^3, slump flow of 880 mm, compressive strength at 28 days of 36 MPa, and thermal conductivity of 0.96 W/mK can be achieved using 100% natural lightweight aggregate. The reuse of waste plastic materials in concretes, which

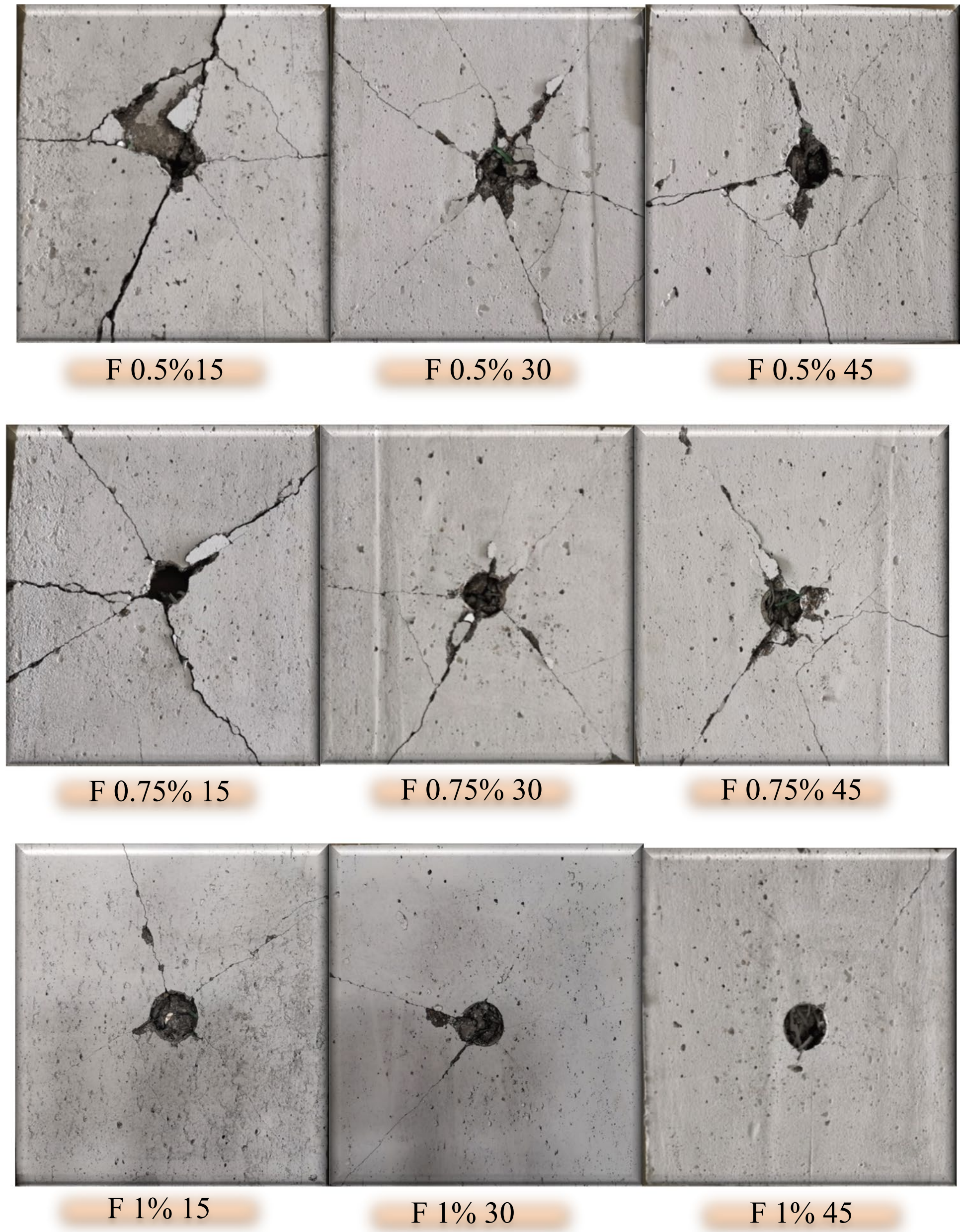

Fig. 30 Failure Pattern of specimens reinforced with PET fiber

can be obtained with a low cost, seems to be a good way, which can contribute to maintain clean environment. In addition, it is clearly from the results of this study that the use of optimum volume fraction and aspect ratio of WPFs improve concrete performance. The details of the above main conclusion can be drawn as follow:

- Uniform SCLC with varying bulk dry densities in the range of 1703–2305 kg/m^3 were produced. SCC mix containing 100% of lightweight aggregates was almost 26% less dry bulk density than SCC with 100% of natural aggregate.
- Although the ultrasonic pulse velocity decreases when lightweight aggregates are incorporated in the mix design of SCC, all the produced SCC and SCLC had UPV values more than 4 km/sec. Thus, the quality of produced concrete can be categorized as good to excellent.
- SCC with 100% crushed gravel aggregates has higher thermal conductivity coefficient than SCLC with replacement level of lightweight aggregates. This difference due to the porous structure of lightweight aggregated, which causes increase in porosity, thus reducing the coefficient of thermal

conductivity Moreover, replacing 40%, 60%, 80%, and 100% lightweight aggregates instead of natural aggregates increased the insulation of the concrete average in ratios of 18.5%, 31.4%, 34.3%, and 46.1%, respectively. This means that energy consumption in the construction would be decreased in ratio up to 46%.

- Concerning dry bulk density, SCLC containing WPF has lower dry bulk density than these of SCLC without PET fiber. There was 8.8% decrease in dry density when the SCLC had a relatively high WPFs content (1%) and high aspect ratio of fiber (45). A decrease in the unit weight of concrete beyond addition PET fiber leads to decrease in the structural dead load.
- The thermal conductivity of SCLC decreased with addition of WPF. The decrease in coefficient of thermal conductivity induced from inclusion PET fiber was in range of 3.1%–18.7% compared to the non-fiber SCLC.
- There was a remarkable influence of PET fiber on the load–deflection curve of SCLC even at 15 aspect ratios, which help to prevent brittle failure of SCLC. Further, the area under curve (T $\frac{D}{150}$) of SCLC increased by increasing volume fraction and aspect ratio of PET fibers. The highest value of T $\frac{D}{150}$ is achieved when volume fraction and aspect ratio of fibers was 1% and 45, respectively. On average, this value increased by almost 181.4% than the one with 0.5% and 15. The SCLC containing WPF exhibited a strain softening with a substantial improve in ductility.
- A substantial enhancement in the low velocity impact strength of all SCLC mixes reinforced with PET fibers over control mix was recorded. The increase in the fibers ratio achieves higher number of blows at first crack, initial scabbing, and failure. Comparing to the control mix, the amount of increasing at ultimate failure varied from (206.6%) at (Vf = 0.5%) to (320%) and (373.3%) for 0.75% and 1% volume fraction.

Declarations

Conflict of interest On behalf of all authors, the corresponding author states that there is no conflict of interest.

Ethical approval This article does not contain any studies with human participants or animals performed by any of the authors.

Informed consent Informed consent was obtained from all individual participants.

References

1. Kılıç A, Duran Atiş C, Yasar E, Özcan F (2003) High-strength lightweight concrete made with scoria aggregate containing mineral admixtures. Cem Concr Res 33:1595–1599
2. Persson B (2001) A comparison between mechanical properties of self-compacting concrete and the corresponding properties of normal concrete. Cem Concr Res 31(2):193–198
3. Okamura H, Ozawa K (1996) Self-compacting high performance concrete. Struct Eng Int J Int Assoc Bridg Struct Eng 6(4):269–270
4. Bansal G (2007) Concrete technology. Indian railways institute of civil engineering, Pune
5. Aggarwal P, Siddique R, Aggarwal Y, Gupta SM (2008) Self-compacting concrete-procedure for mix design. Leonardo Electron J Pract Technol 7(12):15–24
6. De Schutter G et al (2008) Final report of RILEM TC 205-DSC: durability of self-compacting concrete. Mater Struct Constr 41(2):225–233
7. ACI Committee 213 (2003) Guide for structural lightweight aggregate concrete. American concrete institute, Farmington hills, MI, United States
8. ACI commitee 216 (2007) Code requirements for determining fire resistance of concrete and masonry construction assemblies. American concrete Institute
9. EN 206-1 (2000) Concrete-part 1: specification, performance, production and conformity. Europen standards Institution, London
10. "CIP 36-Structural Lightweight Concrete (2003) National ready mixed concrete association, NMRCA
11. Mohammed JH, Hamad AJ (2014) Materials, properties and application review of Lightweight concrete. Tech Rev Fac Eng Univ Zulia 37(2):10–15
12. Karamloo M, Mazloom M, Payganeh G (2017) Effect of size on nominal strength of self-compacting lightweight concrete and self-compacting normal weight concrete: a stress-based approach. Mater Today Commun 13(July):36–45
13. Mehta PK, Monteiro PJM (2006) Concrete: microstructure, properties, and materials. McGraw-Hill, Third edit
14. Madandoust R, Ranjbar MM, Yasin Mousavi S (2011) An investigation on the fresh properties of self-compacted lightweight concrete containing expanded polystyrene. Constr Build Mater 25(9):3721–3731
15. Dev BA, Jayasree S (2016) Effect of lightweight aggregate on the flexural behaviour of self compacting concrete. Int J Sci Eng Res 7(10):16–22
16. ACI commitee 122 (2002) Guide to thermal properties of concrete and masonry systems. American Society for Testing Materials Michigan, PA
17. Sukumar A, John E (2014) Fiber addition and its effect on concrete strength. Int J Innov Res Adv Eng 1(8):144–149
18. M. I. Kaffetzakis and C. G. Papanicolaou (2011) Fiber-reinforced pumice aggregate self-compacting concrete. Concr Eng Excell Effic Prague, Chech Repub
19. Hameed S. Hasan, Abdulkader Ismail Al-Hadithi, Yousif Kh (2022) Yousif, properties of self-compacting lightweight aggregate concrete containing polyolefin fibers. In: 8th International engineering conference on advances in computer and civil engineering towards engineering innovations and sustainability, (IEC-2022), Erbil-Iraq, pp 42–48. https://doi.org/10.1109/IEC54822.2022.9807565
20. Mazaheripour H, Ghanbarpour S, Mirmoradi SH, Hosseinpour I (2011) The effect of polypropylene fibers on the properties of fresh and hardened lightweight self-compacting concrete, The effect of polypropylene fibers on the properties of fresh and

hardened lightweight self-compacting concrete. Constr Build Mater 25:351–358
21. Jankauskaite V, Macijauskas G, Lygaitis R (2008) Polyethylene terephthalate waste recycling and application possibilities: a review. Mater Sci 14(2):119–127
22. Mishra B (2016) A study on use of recycled polyethylene terephthalate (PET) as construction material. Int J Sci Res 5(1):724–730
23. Al-Hadithi AI, Abbas MA (2021) Innovative technique of using carbon fibre reinforced polymer strips for shear reinforcement of reinforced concrete beams with waste plastic fibres. Eur J Environ Civ Eng 25(3):516–537
24. Al-Hadithi AI, Abdulrahman MB, Al-Rawi MI (2020) Flexural behaviour of reinforced concrete beams containing waste plastic fibers. In: IOP conference series: materials science and engineering, 4th international conference on buildings, construction and environmental engineering, BCEE4, 737(15)
25. Alfahdawi IH, Hamid R, Osman SA, Al-Hadithi AI (2018) Modulus of elasticity and ultrasonic pulse velocity of concrete containing polyethylene terephthalate (Pet) waste heated to high temperature. J Eng Sci Technol 13(11):3577–3592
26. Al-Hadithi AI, Al–Ejbari AT, Jameel GS (2013) Behaviour of waste plastic fiber concrete slabs under low velocity impact. Iraqi J Civ Eng 9(1):135–148
27. Al-Hadithi AI, Noaman AT, Mosleh WK (2019) Mechanical properties and impact behavior of PET fiber reinforced self-compacting concrete (SCC). Compos Struct 224:111021
28. De Silva S, Prasanthan T (2019) Application of recycled PET fibers for concrete floors. Engineer 52(01):21–27
29. Tahwia AM, Heniegal AM, Abdellatief M, Tayeh BA, Abd Elrahman M (2022) Properties of ultra-high performance geopolymer concrete incorporating recycled waste glass. Case Stud Constr Mater 17:e01393
30. Tahwia AM, Abdellatief M, Bassioni G, Heniegal AM, Abd Elrahman M (2023) Influence of high temperature exposure on compressive strength and microstructure of ultra-high performance geopolymer concrete with waste glass and ceramic. J Mater Res Technol 23(01):5681–5697
31. Iraqi Standard Specification (IQS No.5:1984) (1984) Cement standard for Portland cement
32. ASTM C618 (2012) Standard specification for coal fly ash and raw or calcined natural pozzolan for use in concrete. American society for testing and material
33. Rizwan SA, Bier TA (2012) Blends of limestone powder and fly-ash enhance the response of self-compacting mortars. Constr Build Mater 27(1):398–403
34. ASTM C33 (2013) Standard specification for concrete aggregates. American society for testing and material
35. ASTM C330 (2017) Standard specification for lightweight aggregates for structural concrete. American society for testing and material
36. ASTM C494 (2013) Standard specification for chemical admixtures for concrete. American society for testing and material
37. Mhedi NM (2019) Evaluation of adding waste plastic fibers on ductility of modifiedfoamed concrete. M.Sc thesis, University of Anbar/college of engineering
38. EFNARC (2005) The European guidelines for self-compacting concrete: specification, production and use
39. Zeyad AA, Saba AM (2017) Influence of fly ash on the properties of self-compacting fiber reinforced concrete. Glob J Res Eng 3(01):1–8
40. Pannem R, Kumar PP (2019) Comparative study of self-compacting concrete containing lightweight and normal aggregates. Slovak J Civ Eng 27(2):1–8
41. ASTM C567 (2014) Standard test method for determining density of structural lightweight concrete. American society for testing and materia
42. BS EN 12390-3 (2009) Testing hardened concrete. Compressive strength of test specimens. British standards institution London, UK
43. ASTM C597 (2009) Standard test method for pulse velocity through concrete. American society for testing and material
44. Penelope A-R, Williams J (2008) Farr's physics for medical imaging, Second edi. Saunders Elsevier
45. ASTM C1113 (1990) Test method for thermal conductivity of refractories by hot wire (Platinum resistance thermometer technique). American society for testing and material
46. ASTM C1609 (2012) Standard test method for flexural performance of fiber-reinforced concrete (Using beam with third-point loading). American Society for Testing and Material
47. ACI commitee 544 (2002) State of the art report on fiber reinforced concrete reported (ACI 544.1 R-96 Reapproved 2002)
48. Bozkurt N (2014) The high temperature effect on fibre reinforced self compacting lightweight concrete designed with single and hybrid fibres. Acta Phys Pol A 125(2):579–583
49. Whitehurst EA (1951) Soniscope tests concrete structures. J Proc 47(2):433–444
50. Penelope A-R, Williams J (2008) Farr's physics for medical imaging, Second ed. Saunders Elsevier
51. Topçu İB, Uygunoğlu T (2010) Effect of aggregate type on properties of hardened self-consolidating lightweight concrete (SCLC). Constr Build Mater 24(7):1286–1295
52. Kurt M, Gül MS, Gül R, Aydin AC, Kotan T (2016) The effect of pumice powder on the self-compactability of pumice aggregate lightweight concrete. Constr Build Mater 103:36–46
53. Yesilata B, Isıker Y, Turgut P (2009) Thermal insulation enhancement in concretes by adding waste PET and rubber pieces. Constr Build Mater 23(5):1878–1882
54. Fraternali F, Ciancia V, Chechile R, Rizzano G, Feo L, Incarnato L (2011) Experimental study of the thermo-mechanical properties of recycled PET fiber-reinforced concrete. Compos Struct 93(9):2368–2374
55. Faisal SK, Irwan JM, Othman N, Ibrahim MHW (2016) Flexural toughness of ring-shaped waste bottle fiber concrete. In: MATEC Web of Conferences, vol 47, p 1002
56. Borg RP, Baldacchino O, Ferrara L (2016) Early age performance and mechanical characteristics of recycled PET fibre reinforced concrete. Constr Build Mater 108:29–47